Journal of Virology – in press

The transmembrane domain of the adenovirus E3/19K protein acts as an ER retention signal and contributes to intracellular sequestration of MHC class I molecules

Running title: E3/19K transmembrane domain as ER retention signal

Martina Sester[1, 2], Zsolt Ruszics[1, 3], Emma Mackley[1], and Hans-Gerhard Burgert[1,#]

[1]School of Life Sciences, University of Warwick, Coventry, CV4 7AL, UK; [2]Department of Transplant and Infection Immunology, Saarland University, 66421 Homburg, Germany; [3]Max von Pettenkofer-Institute, Department of Virology, Genzentrum of the Ludwig Maximilian Universität, Feodor Lynen Str. 25, 81377 Munich, Germany.

[#]Corresponding author: Dr. Hans-Gerhard Burgert, School of Life Sciences, University of Warwick, Coventry, CV4 7AL, UK; Tel.: +44-2476-524-744; E-mail: H-G.Burgert@warwick.ac.uk

Word count abstract: 250

Word count text: 7680

Abstract

The human adenovirus E3/19K-protein is a type-I transmembrane glycoprotein of the endoplasmic reticulum (ER) that abrogates cell-surface transport of MHC class-I (MHC-I) and MICA/B-molecules. Previous data suggested that E3/19K comprises two functional modules: a luminal domain for interaction with MHC-I and MICA/B-molecules, and a di-lysine motif in the cytoplasmic tail that confers retrieval from the Golgi back to the ER. This study was prompted by the unexpected phenotype of an E3/19K-molecule that was largely retained intracellularly despite having a mutated ER-retrieval motif. To identify additional structural determinants responsible for ER-localization, chimeric molecules were generated containing the luminal E3/19K-domain and the cytoplasmic and/or transmembrane domain (TMD) of the cell-surface protein MHC-I K^d. These were analysed for transport, cell-surface expression and impact on MHC-I/MICA/B down-regulation. Similar to the retrieval mutant, replacing the cytoplasmic tail of E3/19K allowed only limited transport of the chimera to the cell surface. Efficient cell-surface expression was only achieved by additionally replacing the TMD of E3/19K with that of MHC-I, suggesting that the E3/19K-TMD may confer static ER-retention. This was verified by ER-retention of an MHC-I K^d molecule with the TMD replaced by that of E3/19K. Thus, we have identified the E3/19K TMD as a novel functional element that mediates static ER-retention, thereby increasing its ER-concentration. Remarkably, the ER-retrieval signal alone without E3/19K-TMD did not mediate efficient HLA-down regulation, even in the context of infection. This suggests that the TMD is required together with the ER-retrieval function to ensure efficient ER-localization and transport inhibition of MHC-I and MIC-A/B-molecules.

22 **Introduction**

23 Human adenoviruses (Ads) can cause a variety of acute diseases (1) but can also persist for
24 variable length of time in a clinically inapparent state (2). More than 50 different Ad serotypes
25 are distinguished and classified in six different species A-F (3). Ads devote a considerable part
26 of their genome to immune evasion functions that facilitate infection and/or maintain a state
27 of balance during persistence or latency (1, 4). If this balance is perturbed as in
28 immunosuppressed patients serious or life-threatening disease may ensue (5). Ads are also
29 widely used as vectors for vaccination and gene therapy (6). Thus, a better understanding of
30 their interaction with the immune system has major medical implications.

31 Many of the Ad immune evasion genes are grouped together in the early transcription unit 3
32 (E3) that is non-essential for virus replication *in vitro* but is preserved in all human Ads (4, 7).
33 This suggests an important role *in vivo*, which is supported by various *in vivo* models (1, 8, 9).
34 E3 proteins counter a variety of immune responses (4, 7, 10), including antigen presentation
35 and natural killer (NK) cells (11). In this context, E3/19K has a dual function. It prevents
36 transport of newly synthesized major histocompatibility class I molecules (MHC-I; HLA in
37 humans) to the cell surface thereby interfering with peptide presentation to cytotoxic T cells
38 (CTL) (12-15). E3/19K also suppresses recognition by natural killer cells via intracellular
39 sequestration of the stress-induced MHC-I related chain A and B (MICA/B) (11) that serve as
40 ligands for the major activating NK receptor, NKG2D (16).

41 E3/19K proteins are type I transmembrane glycoproteins that are expressed by species B-E
42 Ads. Despite their common function, their sequence homology is poor (4, 10, 17, 18). The
43 mature Ad2 protein consists of 142 amino acids forming a luminal domain of ~104 amino acids

44 with two N-linked high-mannose carbohydrates, a transmembrane segment of ~23 amino
45 acids, and a 15-amino-acid-long cytoplasmic tail. E3/19K appears to combine two functional
46 entities to block cell surface display of MHC-I and MICA/B: i) the luminal domain that binds
47 newly synthesized HLA-I molecules, and ii) a di-lysine motif in the cytoplasmic tail that
48 mediates ER retrieval of E3/19K/MHC-I complexes from the *cis*-Golgi back to the endoplasmic
49 reticulum (ER) (12, 13, 19-21).

50 The structural requirements of Ad2 E3/19K for MHC-I and MICA/B binding are well
51 characterised and include two crucial intramolecular disulfide bonds, and a number of other
52 conserved amino acids within the luminal domain (22-26). Most recently, detailed insight into
53 the interaction between the luminal E3/19K domain and a soluble form of HLA-A2 was
54 provided by crystallisalization (26). However, the roles of the transmembrane domain (TMD)
55 and cytoplasmic tail in this process remain controversial. Whilst complex formation can clearly
56 be demonstrated *in vitro* in their absence (22, 27, 28), studies *in vivo* within cells suggested
57 that the interaction is reduced or even abrogated upon deletion of the cytoplasmic tail or the
58 TMD, respectively (13, 28-30). Due to the lack of appropriate antibodies it remained unclear
59 whether this was caused by secondary structural alterations in the luminal domain induced by
60 the deletions or reflected a mere need for membrane anchoring mediated by the TMD (27, 28,
61 31). Also, the exact mechanism of ER localization is not completely understood. While deletion
62 analysis of the cytoplasmic tail and the analysis of E3/19K reporter chimera clearly identified a
63 di-lysine motif important for ER retrieval (4, 13, 19-21, 29, 32), these studies are complicated
64 due to the fact that the efficacy of ER retrieval by di-lysine motifs depends on sequence
65 context (33). When the structural requirements for ER localisation were studied in the context

66 of E3/19K itself, conflicting data were obtained (29, 30), suggesting that other structural
67 elements within the E3/19K protein may be responsible for ER retrieval.

68 The present study was prompted by the phenotype of an E3/19K molecule with a mutated di-
69 lysine retrieval motif. As expected, this mutant reached the cell surface, yet the great majority
70 remained in the ER. Thus, elements in the mutated protein other than the ER retrieval signal
71 clearly contributed to ER retention. By analyzing a series of chimeric molecules in which the
72 cytoplasmic and TMD of E3/19K were replaced individually or in combination with
73 corresponding domains of the *bona-fide* murine cell surface molecule MHC-I K^d we provide
74 evidence that the E3/19K TMD acts as signal for static ER retention that significantly enhances
75 HLA complex formation. Thus, we have discovered a new functional element in E3/19K and
76 propose that efficient transport inhibition of HLA and MICA/B requires the combined activity of
77 an ER retention signal in the E3/19K TMD and the ER retrieval signal in its cytoplasmic tail.

78 ## Material and Methods

79 **Construction of E3/19K and K^d mutant proteins**

80 The Ad2 *Eco*RI D fragment (2674 bp; nucleotides 27,372-30,046bp of the Ad2 reference
81 sequence) containing the E3/19K gene was ligated into pBluescript II KS- (Stratagene), yielding
82 pBS-*Eco*RI D. All mutants were introduced using PCR-mediated mutagenesis essentially as
83 described (24). Generally, each construct was designed using mutant oligonucleotide pairs
84 encompassing the desired sequence alteration in combination with respective flanking
85 primers. For construction of the E3/19K-K^d chimera EEK and EKK a three step protocol was
86 used, separately amplifying E3/19K sequences with K^d compatible ends using pBS-*Eco*RI D as
87 target DNA and the corresponding K^d domains using a K^d cDNA vector pSV-K^d (34) as template.
88 The last step comprised combination of the two PCR products followed by PCR with flanking
89 oligonucleotides. Constructs EKE and EKE* were constructed similarly, but using EKK as
90 template DNA to amplify a 5' fragment. In two independent reactions the corresponding 3'
91 fragments using either wild-type or mutated (EEE*) pBS-*Eco*RI D fragment as template DNA
92 were generated. These PCR fragments were cleaved with *Bsr*GI and *Bcl*I and ligated into wild-
93 type pBS-*Eco*RI D cleaved with the same enzymes.

94 The K^d gene containing the TMD of E3/19K (KEK) was generated by subcloning an 810bp
95 *Apa*I/*Nsi*I fragment of the genomic clone p191.6 of the murine K^d (35), into appropriately
96 cleaved pGEM7+ (Promega) resulting in pKKK-AN. The sequence corresponding to the
97 transmembrane domain of Ad2 E3/19K (nucleotides 29175-29243 of the Genbank Ad2
98 reference sequence) was amplified with flanking primers using pBS-*Eco*RI D as template. The
99 E3/19K specific primers were flanked with 5' homologies to the upstream (3388-3397) and the

100 downstream (3466-3472) K^d coding sequences (numbering is according to the published K^d
101 gene sequence (35). This E3/19K amplicon was first fused to an upstream K^d amplicon using
102 appropriate primers and p161.6 as template. The K^d-E3/19K hybrid TMD amplicon was then
103 fused in another assembly PCR to a downstream K^d specific amplicon generated using relevant
104 primers with p191.6 as template. The final fusion amplicon produced by the flanking K^d primers
105 was restricted with *Sac*I and inserted into *Sac*I-digested pKKK-AN replacing its small original
106 *Sac*I fragment to yield pKEK-AN. pKEK-AN was then inserted into appropriately cleaved p191.6.
107 All intermediates as well as the final construct were verified by sequencing. The sequences of
108 the oligonucleotides used for construction of the various chimeric molecules are available
109 upon request. The generation of KKE has been previously described (36).

110 **Cell lines, culture conditions, and transfections**

111 Transfection of 293 cells (ATCC CRL 1573) with the wild-type and mutant Ad2 *Eco*RI D and
112 *Eco*RV C fragments (encoding the E3A and entire E3 region, respectively) led to the
113 establishment of 293.12, 293E22.7 and 293E3-45 cell lines constitutively expressing wild-type
114 E3/19K (12, 37). 293 cells expressing Ad5 E1A and E1B genes were specifically used to provide
115 the E1A transactivating function for the Ad E3 promoter present in the transfected *Eco*RV C
116 and *Eco*RI D fragments. This system has previously been shown to yield good expression levels
117 of E3 genes (23, 37). The mutant E3/19K cell lines were established by transfection of 293 cells
118 with mutated *Eco*RI D fragments and the neomycin-phosphotransferase gene essentially as
119 described (23, 24). 293K^d2 and 293.12K^d8 were generated by transfection of 293 and 293.12
120 cells, respectively, with a genomic clone of the murine H-2K^d gene (14). 293KKE, previously
121 termed 293KdE3, expresses a K^d molecule with its cytoplasmic tail replaced by that of E3/19K
122 (36). Similarly, cells expressing K^d molecules with the TMD of E3/19K (KEK) were established.

123 293 cells were grown in complete Dulbecco's modified Eagle's medium (DMEM) containing
124 10% fetal calf serum (FCS), 2 mM glutamine and antibiotics. For routine culture, the medium of
125 the transfectants was supplemented with 200µg/ml of active G418 (Calbiochem). K562 is an
126 erythroleukemia cell line lacking MHC class I expression (ATCC CCL243) that was grown in
127 complete RPMI. Cell lines K562-EEE and K562-EEK, derived from K562 by transfection of
128 constructs EEE and EEK, respectively, were cultured in complete RPMI supplemented with 600
129 µg/ml of G418.

130 **Construction of recombinant adenoviruses expressing mutant E3/19K proteins**

131 In order to study mutant E3/19K proteins EEE*, EKE, and EKE* in the virus context, the wild-
132 type Ad2 genome cloned as bacterial artificial chromosome (BAC) (38) was modified in a two-
133 step mutagenesis procedure, essentially as described (39). First, the modified E3/19K
134 sequences from the corresponding pBS-*Eco*RI D plasmids were transferred to pBS-*Eco*RV C (37)
135 containing the Ad2-*Eco*RV C fragment (encompassing the entire E3 region) that had previously
136 been labelled at its unique *Swa*I site by a PCR amplified kanamycin resistance gene (Kn^R)
137 derived from pGPS1.1 (NEB). Next, the *Eco*RI fragments of these constructs containing the
138 E3/19K mutation and the *Swa*I flanked kanamycin (Kn^R) cassette were transferred to the Ad2-
139 BAC by homologous recombination as described earlier (38, 39). Likewise, the wild-type E3
140 sequence was replaced by an *Eco*RI fragment of an unmodified Kn^R labelled construct as
141 control (EEE). After selection of recombinant BACs by kanamycin the resistance cassettes were
142 removed from each construct by *Swa*I treatment followed by re-circularisation with T4 DNA
143 ligase (New England Biolabs). The repaired mutant BACs were re-transformed into *E. coli*,
144 screened for the loss of the Kn^R cassette and sequence-verified across the mutation and
145 recombination site. Modified viruses (Ad2-EEE, Ad2-EEE*, Ad2-EKE, Ad2-EKE*) were

146 reconstituted from the corresponding BACs upon transfection of 293 cells with purified BAC
147 DNA as described (38).

148 **Monoclonal antibodies and antisera**

149 The following monoclonal antibodies (mAbs) were used in this study: W6/32, anti-HLA-A,-B,
150 and -C (ATCC HB95); BB7.2, anti-HLA-A2 and -Aw69 (40); BAMO3, anti-MICA/B (41); Tw1.3 (13)
151 (kindly provided by J. Yewdell, NIH), 3A9 and 3F4 (42), anti-E3/19K. The polyclonal antisera C-
152 tail (23) and Kc-tail (36) recognize the cytoplasmic tails of E3/19K and K^d, respectively.

153 **Cell labeling, immunoprecipitation, and SDS-PAGE, endoglycosidase H treatment**

154 Labeling of cells with ^{35}S-methionine, immunoprecipitation of NP40 extracts, sodium dodecyl
155 sulfate-polyacrylamide gel electrophoresis (SDS-PAGE), and endoglycosidase H (endo H)
156 treatment were carried out essentially as described (12, 23, 43).

157 **Flow cytometry analysis**

158 For detection of antigens, unfixed cells were incubated with the mAbs given above followed by
159 goat anti-mouse IgG conjugated with fluorescein isothiocyanate (Sigma) or Alexa 488
160 (Invitrogen) as described (23, 24), except that for internal staining of antigens 0.075% saponin
161 (Sigma) was used. For the last two washes and for analysis, saponin was omitted from the
162 buffer. As demonstrated previously (23, 24), staining in the presence of the mild detergent
163 saponin allows access of Abs to the ER lumen preserving ER membrane proteins while
164 concomitantly extracting a large fraction of cell surface proteins. This treatment therefore
165 primarily detects intracellular proteins, and the values obtained with the saponin treatment
166 were used as the denominator in the ratios (cell surface/internal) determined in Figs. 2B, 8B,
167 and 9.

168 **Immunofluorescence**

169 Immunofluorescence was principally performed as described (44) with the modifications
170 indicated below. Cells were fixed for 10 min in 3% paraformaldehyde (Sigma) in PBS and
171 washed two times with PBS. Internal staining was achieved by permeabilising the cells for
172 5 min with 0.5% Triton-X-100/PBS. Nonspecific binding sites were blocked for 30 min with 1%
173 BSA/PBS. This buffer composition was kept throughout the following incubation and washing
174 steps. Primary antibody 3A9 (42) was applied for 1 hour as a 1:5 dilution of cell culture
175 supernatant. Cy3-conjugated secondary goat anti-mouse IgG (Dianova) was used in a 1:200
176 dilution. Preparations were embedded with Vectashield (Serva) and viewed with a confocal
177 microscope (Leica CLSM TCS4D) equipped with a crypton-argon laser. Data were recorded and
178 processed using implemented software (Leica).

179 ## Results

180 **Constructs and cell lines utilized to identify the domains that contribute to intracellular**
181 **localization of E3/19K**

182 To identify the structural elements that contribute to intracellular sequestration of E3/19K and
183 HLA, site directed mutagenesis and domain swapping was employed to systematically
184 manipulate the TMD and/or cytoplasmic tail of the Ad2 E3/19K protein (Fig. 1, EEE). Mutation
185 of the di-lysine motif at positions 139/140 of E3/19K by serine is denoted by an asterisk (*). In
186 addition, the TMD (EKE, EKE*) and/or the cytoplasmic tail of E3/19K (EKK, EEK) were replaced
187 by those of the murine MHC-I molecule K^d (Fig. 1, KKK). This MHC-I allele was chosen as a
188 control for the distribution of a typical cell surface protein since it allowed us to monitor the
189 presence and correct folding of individual domains in the mutant constructs due to the
190 availability of antibodies to various portions of E3/19K and K^d. All mutations were introduced
191 into the *Eco*RI D fragment of Ad2. In doing so, the known Ad-specific control elements, such as
192 the promoter, donor and acceptor splice sites, translation regulatory elements and poly(A)
193 signals were retained. The mutagenized Ad2 fragments were transfected into 293 cells
194 together with the neomycin resistance gene. A total of 25–30 cell clones derived from each
195 transfection were screened initially for expression of the E3/19K constructs by quantitative
196 FACS analysis in the presence of the detergent saponin. Clones with similar E3/19K expression
197 as cells expressing wild-type E3/19K, as verified by immunoprecipitation upon 30-60 min
198 metabolic labelling, were chosen for further analysis. In addition, the relative distribution of
199 mutant proteins on the cell surface and intracellularly was compared with that seen in a cell
200 line constitutively expressing wild-type E3/19K (EEE).

201 **Efficient cell surface expression of E3/19K requires replacement of its transmembrane**
202 **domain**

203 In line with the previous suggestion that the di-lysine motif is the only structural determinant
204 in the E3/19K protein required for inhibition of transport to the cell surface (20, 29, 45),
205 mutation of this motif resulted in cell surface expression of the mutant protein (Fig. 2A, EEE*,
206 lower panel), whereas wild-type E3/19K (EEE) did not reach the cell surface. Remarkably,
207 though, internal staining in the presence of the detergent saponin revealed that the majority of
208 the EEE* protein remains intracellularly (Fig. 2A; compare the mean fluorescence intensity
209 (MFI) 98.5 versus 31.9). An inverse distribution was seen for the *bona-fide* plasma membrane
210 protein MHC K^d (KKK), where the majority of the protein was found on the cell surface (Fig. 2A;
211 55.0 versus 93.2). The histograms shown in Fig. 2A represent typical examples of one cell clone
212 of each transfection. To control for clonal variation, three or more independent clones of each
213 transfection were analysed in at least three different experiments. The relative subcellular
214 distribution of constructs was expressed as the ratio of MFIs obtained in the absence and
215 presence of saponin (Fig. 2B; primarily reflecting cell surface versus internal expression, see
216 Material and Methods). The collective data clearly confirm that EEE* is predominantly localized
217 intracellularly. Therefore, amino acids in the E3/19K protein other than the di-lysine motif in
218 the cytoplasmic tail seem to contribute to intracellular localization. Since replacing the entire
219 cytoplasmic tail of E3/19K protein by that of K^d (Fig. 1, EEK) resulted in a similar distribution as
220 EEE* (Fig. 2A; 89.7 versus 36.0; and Fig. 2B), other elements within the C-terminal portion of
221 E3/19K apart from the di-lysine motif appear to play a minor role for ER retention. Thus,
222 although EEE* and EEK could be detected on the cell surface, the majority of both mutant
223 proteins were localized intracellularly. To assess the impact of additional structural features on
224 intracellular localization, a chimeric E3/19K protein was generated where both the TMD and

225 the cytoplasmic tail were replaced by the respective K^d sequences (EKK, Fig. 1). Interestingly,
226 the distribution of EKK differed drastically from that of EEE* and EEK and was comparable to
227 the staining ratio of the plasma membrane protein KKK (Fig. 2A; 25.2 versus 88.4 and Fig. 2B).
228 These results suggest that the TMD of K^d promotes cell surface expression, and conversely the
229 E3/19K TMD contributes to its efficient intracellular retention. This view was confirmed by the
230 phenotype of a chimeric protein containing the TMD of K^d together with an E3/19K tail where
231 the di-lysine motif was mutated (EKE*, Fig. 1), thus eliminating the impact of ER retrieval.
232 Indeed, EKE* was expressed on the cell surface to a similar extent as the proteins EKK and KKK
233 (Fig. 2A and B). Finally, to more precisely delineate the relative importance of the two
234 structural elements, a chimeric protein bearing the TMD of K^d together with the native E3/19K
235 tail (EKE, Fig. 1) was analysed. As predicted for a protein with a functional di-lysine motif, EKE
236 shows a distribution similar to that of the wild-type E3/19K protein (Fig. 2A and B, compare EEE
237 with EKE). Together, these results demonstrate that both the di-lysine motif and the TMD of
238 the E3/19K protein contribute significantly to its efficient intracellular localization, whereas
239 other amino acids in the cytoplasmic tail are of minor importance for the subcellular
240 distribution.

241 **The subcellular distribution of the chimeric proteins is consistent with their flow cytometry**
242 **phenotype**

243 To confirm the distribution of the constructs between cell surface and intracellular
244 compartments and to obtain more information as to their intracellular localisation,
245 immunofluorescence microscopy was employed in the absence and presence of detergent
246 using mAb 3A9 (42) directed to a formaldehyde-resistant, exposed linear epitope (residue 15-
247 21) of the E3/19K protein (Fig. 3). In line with previous observations, EEE was not detected on

248 the cell surface (Fig. 3A). The same holds true for EKE (Fig. 3F). In agreement with the flow
249 cytometry analysis, EEE* and EEK were detected on the cell surface (Fig. 3B, C); however, their
250 expression was generally weaker than that of EKK or EKE* (Fig. 3D, E). When the same cell lines
251 were fixed and treated with detergent to additionally detect E3/19K in cytoplasmic
252 compartments (Fig. 3G–L), cells expressing EKK and EKE* exhibited primarily a cell surface
253 pattern and little internal staining (Fig. 3J, K). This contrasts dramatically to cell lines expressing
254 wild-type E3/19K that showed a bright reticular staining of the perinuclear region, typical for
255 the ER (Fig. 3G). Likewise, this perinuclear rim of fluorescence was present in cell lines
256 expressing EEE*, EEK and EKE (Fig. 3H, I, L) with EEE* and EEK exhibiting somewhat higher
257 number of vesicular structures. Thus, the chimera may be classified into three groups: proteins
258 with intact di-lysine motif are efficiently localized in the ER (EEE; EKE). Also, proteins containing
259 the native TMD without functional di-lysine motif (EEE*, EEK) are predominantly localized in
260 the ER at steady state, although the presence of vesicular structures and a low cell surface
261 expression indicates transport to other compartments. Finally, a third group of mutants
262 comprises proteins with the capacity to be efficiently transported to the cell surface (EKK,
263 EKE*, and KKK).

264 **Manipulations of the cytoplasmic tail and TMD of E3/19K do not significantly affect the**
265 **conformation of the luminal region**

266 ER retention of EEE* and EEK might be due to misfolding and activation of the unfolded protein
267 response by quality control systems residing in the ER (46). We therefore sought to find
268 potential evidence for misfolding of the E3/19K mutants and chimera by analysing their ability
269 to be recognized by a panel of conformation-sensitive mAbs against the E3/19K protein (42).
270 However, when the various E3/19K constructs were immunoprecipitated from ^{35}S-methionine

271 labelled cells using mAbs 3A9, 3F4 (data not shown), and Tw1.3, no significant change in
272 reactivity relative to wild-type E3/19K was observed, indicating that the conformation of the N-
273 terminal luminal domain of E3/19K present in all constructs did not seem to be grossly altered
274 by changes of the TMD or the cytoplasmic tail. As an example, immunoprecipitation data are
275 shown for the conformation-sensitive mAb Tw1.3 that recognized all mutant proteins of the
276 expected size with similar efficiency (Fig. 4). Wild-type E3/19K contains two carbohydrates of
277 the high mannose type and migrates at approximately 25kDa with some faster migrating
278 species indicative of mannose processing. Accordingly, the predominant ~25kDa protein
279 species of EEE, EEE*, EKE* and EKE represents the fully glycosylated form, whereas the faster
280 migrating minor species (black arrowhead) represent the respective monoglycosylated forms.
281 Due to the different size of the cytoplasmic tail of K^d and E3/19K (40 versus 15 amino acids) the
282 chimeric proteins EEK and EKK exhibit an increase in apparent molecular weight by 2.25 kDa
283 (Fig. 4, lanes 3 and 4). The same results were obtained using antisera against the respective
284 cytoplasmic tails (data not shown). As expected, an antiserum against the C-terminal 11 amino
285 acids of K^d recognized constructs EEK and EKK, while a serum against the C-terminus of E3/19K
286 (C-tail) recognized all other constructs. Thus, the correct apparent molecular weight and the
287 ability of the proteins to be recognized by the corresponding antibodies suggest that all
288 mutants contain the desired sequence alterations. Moreover, the similar efficiency by which
289 Tw1.3 immunoprecipitates the various constructs shows that the alterations introduced into
290 the TMD and cytoplasmic domain do not seem to significantly affect the conformation of the
291 luminal part of E3/19K. Therefore, it is highly unlikely that the predominant intracellular
292 localization of EEE* and EEK is mediated by a quality control system that recognizes and retains
293 unfolded proteins.

294 **Carbohydrate modifications reveal the importance of the TMD and cytoplasmic tail for**
295 **transport inhibition**

296 The wild type Ad2 E3/19K contains two N-linked carbohydrates of the high mannose type
297 characteristic for ER resident proteins (47) whereas glycoproteins that exit the ER may undergo
298 further modifications in post-ER compartments and incorporate complex type carbohydrates.
299 As these processed proteins show a slower electrophoretic mobility in SDS-PAGE, the
300 appearance of these forms represents another means of assessing the ability of the mutant
301 proteins to exit the ER. Such slower migrating protein species are visualized to some extent for
302 EEK and EEE*, but are much more prominent for EKK and EKE*, both containing the TMD of K^d
303 (Fig. 4, lanes 2-5; processed species labelled with a line and asterisk). This conversion to
304 complex type sugars is indicative of transport through the medial/trans Golgi apparatus, which
305 was not seen for E3/19K proteins with intact di-lysine motifs (Fig. 4, EEE and EKE, lanes 1 and
306 6). Quantitation of band intensities revealed that 44% of EKK, 47% of EKE*, 11% of EEK and
307 ~5% of EEE* were processed within the labelling period of 1h (data not shown). Therefore, the
308 mutation of the di-lysine motif principally allows exit of the E3/19K protein out of the ER to the
309 medial Golgi apparatus where it was shown to acquire endoglycosidase H resistant (endo H^R)
310 complex carbohydrates (data not shown), in line with previous data for a secreted E3/19K
311 variant (28). The extent of this processing, and thus the degree of transport through the medial
312 Golgi apparatus, is drastically enhanced by the TMD of K^d (Fig. 4, compare processing of EEE*
313 and EEK with EKK and EKE*). This was verified by the acquisition of endo H^R carbohydrates in
314 pulse-chase analysis (data not shown). The limited acquisition of complex type sugars for EEE*
315 and EEK confirmed the immunofluorescence data and strongly suggests that the constructs
316 lacking di-lysine motifs (EEE* and EEK) largely remain in the ER. As this could be caused by
317 complex formation with HLA, we tested whether transport to the cell surface was increased in

318 the absence of HLA molecules. To this end, wild type E3/19K and EEK were stably expressed in
319 K562 cells that lack HLA. While the expression level of these E3/19K constructs was lower in
320 K562 than in 293 cells due to the lack of E1A that transactivates the E3 promoter (Fig. 4B), the
321 absence of HLA-molecules did not result in enhanced cell surface transport, as neither
322 construct showed evidence for processing to a higher apparent molecular weight (asterisk in
323 Fig. 4B, lane 2, compare EEK in 293 and K562) nor acquisition of Endo H resistance in pulse
324 chase analyses (Figure 4C). This is consistent with the lack of cell surface expression of both
325 types of transfectants (data not shown). Therefore, we exclude the possibility that HLA
326 complex formation causes ER retention of constructs with mutated di-lysine motifs. Rather, the
327 lack of transport of EEK in K562 cells suggests that the presence of HLA contributes to the
328 limited EEK transport in 293 cells.

329 **The capacity of the E3/19K chimera to bind HLA depends on the nature of the TMD**

330 To assess whether the manipulations of the E3/19K protein would affect its ability to associate
331 with HLA molecules, complex formation was measured by co-immunoprecipitation. HLA
332 antigens were precipitated using mAb W6/32 directed to HLA-A, -B and –C (Fig. 5A). In cells
333 expressing wild-type E3/19K (EEE), E3/19K was co-precipitated as an additional band of 25 kDa
334 that was not present in non-transfected cells (Fig. 5, lanes 1 and 2). E3/19K related protein
335 species of the expected molecular weight were also seen in cells expressing the mutant E3/19K
336 molecules (lanes 3–7). Although the visualization of EKK and EKE* was compromised by the
337 heterogenous nature of the co-precipitated band (see Fig. 4), both proteins were clearly visible
338 in longer exposures (data not shown). Thus, all mutants principally retain the ability of complex
339 formation with HLA molecules. Quantitative phosphoimager analysis of the co-precipitated
340 mutants relative to wild-type E3/19K revealed that complex formation of EEE, EEE* and EEK

341 with HLA is comparable within the 1h labelling period (Fig. 5A, lanes 2–4 and Fig. 5B) whereas
342 the amount of co-precipitating protein is substantially lower in cell lines expressing EKK, EKE*
343 and EKE (Fig. 5A, lanes 5–7 and Fig. 5B). This indicates that the TMD of E3/19K significantly
344 contributes to the efficiency of complex formation with HLA.

345 **Replacement of the E3/19K TMD and cytoplasmic tail dramatically affects the efficiency of**
346 **HLA and MICA/B retention**

347 To determine whether the ability of HLA molecules to interact with the mutant E3/19K
348 constructs correlates with their transport, the carbohydrate processing of HLA molecules was
349 analysed in a pulse-chase experiment (Fig. 6). Stable transfectants and non-transfected control
350 cells were pulse-labelled for 20 minutes, washed and further incubated for 150 min in the
351 presence of an excess of unlabelled methionine. Subsequently, HLA-A2 was first precipitated
352 (Fig. 6A) and thereafter the remaining HLA-A, -B and -C alleles (Fig. 6B). Processing of HLA-A2
353 was analysed separately, since it was shown to have a high affinity for Ad2 E3/19K (22, 48).
354 Furthermore, by analysing only one HLA allele the detection of small changes in apparent
355 molecular weight accompanying the conversion of the single HLA glycan to complex-type
356 sugars in the medial/trans Golgi apparatus becomes more apparent. Precipitated HLA antigens
357 were digested with endoglycosidase H (endo H) which cleaves high mannose sugars resulting in
358 faster migrating species of HLA (HLA-A2^{c}, HLA^{c}) as compared to the HLA species that acquired
359 endo H-resistant, complex carbohydrates in the medial/trans Golgi (HLA-A2^{R}, HLA^{R}).
360 Quantitation of the amount of endo H-resistant protein in the individual cell lines (bottom
361 panels) revealed that processing of HLA antigens in the presence of EKK and EKE* was
362 indistinguishable from that seen in the absence of E3/19K in 293 cells. By contrast, in the
363 presence of wild-type E3/19K (EEE), EEE* and EKE essentially all HLA-A2 molecules remained

364 endo H sensitive and thus contained high mannose type sugars. Similar results were obtained
365 for the processing of the remaining lower affinity HLA alleles (Fig. 6B), except for EEK and
366 particularly EKE expressing cells. In cells expressing EEK, a considerably larger proportion of
367 HLA molecules acquired endo H resistance as compared to the EEE* transfectant. This is not
368 reflected in the distribution of the two E3/19K constructs themselves (Fig. 2B), indicating that
369 amino acids in the cytoplasmic tail of E3/19K other than the di-lysine motif may not affect their
370 transport, but may have an influence on the interaction with MHC class I molecules. The
371 phenotype of EKE is surprising considering the presence of the native E3/19K retrieval signal
372 but is consistent with its reduced complex formation with HLA-A, -B and -C alleles observed in
373 co-precipitation experiments (Fig. 5) and the generally lower binding affinity of HLA B and C
374 alleles to E3/19K (25, 48).

375 Finally, the steady state cell surface expression of HLA and MICA/B was quantitatively
376 determined using flow cytometry. At least three different cell clones derived from each
377 transfection were analysed using mAb W6/32 (Fig. 7A). The HLA expression level of 293 cells
378 and three G418-resistant, E3/19K negative cell lines was set as 100%. The results confirm the
379 data obtained from co-precipitation and pulse-chase analysis. As previously shown, HLA cell
380 surface expression is drastically reduced in the presence of wild-type E3/19K (EEE). In line with
381 the pulse-chase experiments, the removal of the ER retrieval signal in EEE*and EEK alleviates
382 the transport block whereby HLA cell surface expression reached considerably higher levels in
383 EEK as compared to EEE* expressing cell lines (reduction by 34% versus 66%). Some reduction
384 of HLA expression (by approximately 25%) was visible in EKK transfectants whereas cell lines
385 expressing EKE* exhibited normal HLA levels. Remarkably, despite the presence of the ER
386 retrieval signal in EKE, HLA cell surface expression at steady state is only slightly suppressed in
387 such cell lines, consistent with the reduced ability to interact with HLA molecules and the

388 ability to acquire endo H resistance. Expression of HLA-A2 on the plasma membrane correlated
389 with the pulse-chase results (data not shown). Of note, the cell surface pattern for MICA/B, the
390 other known target molecule of E3/19K, was largely similar in these transfectants (Fig. 7B). This
391 indicates that down regulation of both MICA/B and MHC-I similarly depends on the TMD and
392 cytoplasmic tail of E3/19K.

393 **The E3/19K TMD actively suppresses cell surface expression of a *bona fide* plasma membrane**
394 **protein**

395 The data above show that the MHC-I TMD promotes cell surface expression of E3/19K and
396 conversely the E3/19K TMD has features that contribute to ER retention of E3/19K and HLA. To
397 directly investigate whether the TMD alone is sufficient to promote ER retention and suppress
398 cell surface expression of a heterologous *bona fide* plasma membrane protein, the K^d TMD was
399 substituted by that of E3/19K to yield KEK (Fig. 1). Stable 293 transfectants were screened for
400 expression of KEK by flow cytometry in the presence and absence of saponin using mAbs
401 SF1.1.1 and 34-1-2 directed to the α3 and α1/2 domain of K^d, respectively. Successful
402 immunoprecipitations with 34-1-2 and antibodies directed to the cytoplasmic tail of K^d (C-tail)
403 confirmed the presence of the respective domains in KEK and the expected molecular weight
404 (Fig. 8A). Non-transfected 293 cells and KEK-negative, G418-resistant cell clones, such as K1,
405 exhibited only background bands. As shown in Fig. 8B, KEK expressing cell clones exhibited a
406 drastically reduced cell surface expression and concomitantly an increased intracellular
407 staining relative to wild-type K^d (KKK), very similar to that of K^d in cells co-expressing wild-type
408 E3/19K (KKK+EEE). As expected, cell surface expression of a hybrid K^d molecule with its
409 cytoplasmic tail replaced by that of E3/19K showed an exclusively intracellular localisation

410 (KKE, Fig. 1 and Fig. 8B). The surface expression of other typical cell surface molecules such as
411 CD46 or HLA was not significantly affected by KEK expression (data not shown).

412 Taken together, this demonstrates that the TMD of E3/19K can dominantly convert a plasma
413 membrane protein into an intracellular protein and thus contains features that favour
414 intracellular localisation/ER retention. Comparative pulse-chase analyses of KEK and KKE with
415 wild-type K^d in the presence and absence of E3/19K (KKK+EEE and KKK, respectively) clearly
416 indicated that both constructs are retained in the ER. Unlike wild-type K^d (KKK) that shows the
417 typical processing associated with the acquisition of complex type sugars (Fig. 8C, lanes 4-6, *),
418 KEK and KKE failed to acquire complex type sugars, similar to wild-type K^d in the presence of
419 E3/19K (KKK+EEE; Fig. 8C, compare lanes 7-12 with 1-3). The progressively lower apparent
420 molecular weight of the chased K^d molecule reflecting mannose trimming in the ER, and the
421 drastically enhanced complex formation with the 100 and 110 kDa species of the amyloid
422 precursor-like protein 2 (APLP2, Fig. 8C, compare lanes 7-12 with 1-3) which is known to occur
423 when transport of K^d out of the ER is inhibited, e.g. by co-expression of E3/19K (36) provides
424 independent evidence for ER localisation of KEK, KKE and K^d in the presence of E3/19K. The
425 close correlation between APLP2 co-immunoprecipitation and ER localisation is confirmed by
426 the loss of association of the two APLP2 species upon transport of K^d out of the ER and
427 acquisition of complex type sugars during the chase period (Fig. 8C, lanes 4-6).

428 **ER retention by the E3/19K TMD also occurs during virus infection**

429 To assess the physiological relevance of our findings, the functional activity of the newly
430 discovered ER retention signal in the E3/19K TMD was analyzed during viral infection. To this
431 end, the E3/19K mutants EEE*, EKE* and EKE were introduced into the Ad2 genome using
432 recombineering (38, 39). HeLa cells (data not shown) and 293 cells were infected with wild-

433 type Ad2, Ad2 viruses expressing the modified E3/19K molecules, and Ad2 dl810, an Ad2
434 lacking all E3 genes as negative control (49) (data not shown). As indicated by the ratios of cell
435 surface expression and internal staining, the distribution of the mutant E3/19K molecules (Fig.
436 9A) and HLA target molecules (Fig. 9B) was essentially the same as in the transfection system
437 (Fig. 2 and 7). Wild-type E3/19K (EEE) and EKE were exclusively found intracellularly, whereas
438 some cell surface expression and an increased ratio was seen for EEE*. Remarkably, Ad2
439 mediated expression of EKE* resulted in a ratio typical for a cell surface protein. The HLA
440 expression profile was consistent with that of the transfected cell lines (Fig. 7) and correlated
441 with that of the E3/19K mutant constructs except for EKE, where down regulation of HLA was
442 only modest, even though EKE was completely intracellular. Thus, the results obtained by the
443 transfection system used here for most experiments were essentially reproduced during virus
444 infection, suggesting that the newly discovered functional activities of the TMD are
445 physiologically relevant.

446 **Discussion**

447 The adenovirus E3/19K protein subverts recognition of T cells and NK cells by retaining MHC-I
448 and MICA/B molecules in the ER (11, 12, 15, 24). To date, this capacity was thought to be
449 based on the combined action of two functional entities, the ER luminal domain that binds to
450 MHC-I and MICA/B, and an ER retrieval signal in the cytoplasmic tail that mediates retrograde
451 transport of E3/19K with its attached target molecules from the ERGIC/*cis* Golgi to the ER (20,
452 21, 28, 29). In this study, we show that the TMD of E3/19K represents an additional functional
453 element that crucially contributes to both efficient ER localisation of E3/19K and down
454 regulation of target molecules. This conclusion was reached by analyzing a series of chimeric
455 constructs that contained the luminal domain of E3/19K together with the TMD and/or
456 cytoplasmic tail of the *bona-fide* plasma membrane protein MHC-I K^d. Analysis of these
457 E3/19K-MHC-I chimera revealed the importance of the E3/19K TMD in this process, since its
458 replacement led to high cell surface expression. Conversely, replacement of the TMD of K^d by
459 that of E3/19K was sufficient to cause ER retention showing its dominant activity. Based on
460 these data, we propose that the TMD of E3/19K mediates static ER retention. Consistent with
461 this conclusion, the TMD contributes significantly to the binding and retention of HLA-I and
462 MICA/B, as its replacement severely compromised the down regulation of these molecules.

463 Figure 10 illustrates the transport characteristics of the various E3/19K molecules and HLA, and
464 summarises the overall efficiency of HLA-I down-regulation. Chimera with similar phenotypes
465 are grouped together. In wild-type E3/19K (EEE), the ER retrieval signal and the ER retention
466 signal of the TMD act in concert to maintain a high concentration of E3/19K in the ER where it
467 efficiently associates with its target molecules (Fig. 10A). Without ER retrieval signal, but in the
468 presence of the cognate E3/19K TMD (Fig. 10B, EEE* and EEK) the bulk of these constructs

469 remains in the ER through static ER retention and only a small fraction of E3/19K-HLA
470 complexes is further transported to the cell surface. The predominant intracellular retention of
471 these constructs is not caused by complex formation with HLA in the ER as there was no
472 transport in HLA-negative cells. The higher HLA cell surface expression observed for EEK
473 expressing cells versus EEE* may suggest that residues in the cytoplasmic tail other than the ER
474 retrieval signal may impact on the efficiency of HLA down regulation as previously suggested
475 (29). In the absence of both the di-lysine motif and the E3/19K TMD (Fig. 10C, EKK and EKE*)
476 there is no static ER retention, and consequently large amounts of chimeric proteins rapidly
477 exit the ER. Due to the lack of an ER retrieval signal, these constructs are further transported
478 through the Golgi to the cell surface. Thus, these constructs have a distribution and cell surface
479 expression comparable to that of typical surface proteins, such as K^d. It is unclear to what
480 extent EKE* and EKK reach the cell surface in complex with HLA molecules. Co-
481 immunoprecipitation of these constructs is substantially lower than for wild-type E3/19K and
482 the other mutants with native E3/19K TMD. However, these constructs can still be co-
483 precipitated after 1h of chase (data not shown) indicating that a considerable fraction of
484 EKK/EKE* remains associated with HLA during transport to and possibly on the cell surface. As
485 expected, no cell surface expression was demonstrated for EKE that due to the absence of the
486 E3/19K TMD is rapidly transported from the ER to the ERGIC/*cis* Golgi, but is also efficiently
487 returned to the ER owing to the presence of the ER retrieval signal (Fig. 10D). Surprisingly, this
488 was not the case for the majority of HLA-I and MICA/B molecules in those cells, as those were
489 transported further to the cell surface. This suggests that complexes with EKE that reach the
490 ERGIC/*cis*-Golgi compartment are prone to dissociation releasing HLA and MICA/B molecules
491 for transport to the cell surface (Fig. 10D). Conversely, the E3/19K TMD seems to prevent rapid
492 ER export and hence dissociation, and thus contributes to efficient HLA down regulation. Viral

493 infection with corresponding Ad2 mutants confirmed the important functional contribution of
494 the TMD and the cytoplasmic tail. Taken together, this model can explain the transport
495 characteristics of the chimera and their effect on HLA cell surface expression. Accordingly, it is
496 the combination of static ER retention provided by the polar TMD and ER retrieval by the di-
497 lysine motif that brings about efficient HLA and MICA/B down modulation.

498 Our findings with EEK and EEE* are in line with previous studies using C-terminally deleted
499 E3/19K proteins, which also showed cell surface expression (13, 29). However, as the
500 intracellular expression was not concomitantly quantified, those studies did not provide any
501 information as to the relative distribution of constructs on the cell surface versus intracellular
502 compartments (13, 19, 29). Moreover, the previous studies did not specifically assess the role
503 of the TMD. Deletion analyses have shown that E3/19K mutants truncated within the luminal
504 domain (at residue 96) adjacent to the TMD or within the TMD did not exhibit any interaction
505 with HLA and were secreted. By contrast, constructs truncated C-terminal of the TMD within
506 the cytoplasmic tail associated with HLA and were expressed on the surface (28, 31). This may
507 suggest that *in vivo* the luminal domain alone without TMD or cytoplasmic tail is insufficient for
508 HLA interaction. However, in those studies it could not be ruled out that misfolding, e.g. due to
509 inappropriate disulfide bond formation, was the potential cause for the loss of complex
510 formation. Furthermore, it remained open as to whether the TMD was required as a mere
511 membrane anchor or had additional functions. By contrast, the conformation of the luminal
512 domains in the constructs generated here does not seem to be significantly altered, as all
513 conformation-dependent mAbs tested showed a similar efficiency in precipitating the mutant
514 E3/19K molecules as compared to wild-type (Fig. 4). This panel of mAbs was shown to be highly
515 sensitive to conformational changes induced by mutations of individual amino acids, small
516 deletions, or disruption of intramolecular disulfide bonds (23, 24, 42, 50). Our data emphasise

517 the crucial importance of the TMD not as a mere membrane anchoring device but rather as a
518 functional module to mediate both static ER retention and a more efficient complex formation
519 with target molecules. In light of our data, the loss of interaction upon deletion of the TMD (28,
520 31) might be explained by the lack of static ER retention and ER retrieval and thus an
521 insufficient concentration of E3/19K in the ER. These *in vivo* data are not necessarily in conflict
522 with the successful interaction of the purified soluble luminal E3/19K domain with HLA *in vitro*,
523 as this may have been forced by the high protein concentrations used in those systems (22, 25,
524 26, 28, 31).

525 Due to the common function of all E3/19K proteins examined to date (7, 12, 17, 25, 51), the
526 specific feature of the TMD, identified here to promote ER retention, should be preserved in
527 E3/19K proteins. However, none of the 20 strictly conserved amino acids of E3/19K is localized
528 in the TMD (24). Also its length is not distinctly different from TMDs of plasma membrane
529 proteins (23 amino acids in E3/19K versus 24 in K^d) (52). A well-conserved property of TMDs of
530 all E3/19K proteins, however, is the unusually high number of polar amino acids. Nine polar
531 residues are present in species C, e.g. in the Ad2 E3/19K protein, 9-12 in species B, 9 in species
532 E, and 4 in species D (4). Therefore, the high number of polar amino acids in the E3/19K TMD
533 could contribute to static ER retention. By contrast, the TMD of K^d used here as *bona fide*
534 plasma membrane protein to replace the corresponding domain of E3/19K contains only two
535 polar residues. Whilst we cannot recognise major differences to TMDs of other typical cell-
536 surface proteins, such as CD4, CD8 or the IL-2 receptor alpha chain (21, 32, 53) used in similar
537 domain-swapping studies, we cannot completely rule out whether those TMDs would give
538 identical results. It will be interesting to mutate the various polar amino acids individually and
539 in combination to elucidate their potential role in this process. Moreover, it is tempting to
540 speculate, whether lower numbers of polar amino acids in TMDs of other E3/19K proteins may

541 in fact be less potent to promote ER retention of target molecules. In support of this, the
542 Ad19a E3/19K protein with four polar amino acids in the TMD is less efficient than Ad2 E3/19K
543 in down-regulating HLA alleles (54). Apart from E3/19K, numerous other proteins have been
544 described where uncharged polar or charged amino acids in the TMD contribute to efficient ER
545 localization or are otherwise involved in transport regulation of protein complexes to the cell
546 surface (46). Examples include the B-cell immunoglobulin receptor (55, 56), cytochrome P450
547 (57, 58), and the ER resident protein UDP-glucuronosyl transferase (GT) (59). Interestingly,
548 similar to E3/19K, the latter contains a di-lysine motif, the mutation of which does also not
549 affect the predominant ER localization (57). In addition, various viral proteins have been
550 reported where ER localisation is mediated by TMDs, although in many cases ER retention is
551 more complex as it involves multiple TMDs, e.g. the E1 and E2 complexes of hepatitis C virus
552 and rubella virus (60, 61). In both cases these represent viral envelope proteins that have to
553 assemble in the ER to mediate virus budding or are retained individually to avoid export of
554 unassembled protein complexes. In light of the striking polarity of the E3/19K TMD, this quality
555 control mechanism may have been exploited for the immune evasion function of E3/19K in
556 that it guarantees a high local concentration in the ER membrane for efficiently sequestrating
557 HLA and MICA/B.

558 We cannot rule out the possibility that the E3/19K TMD, apart from increasing the local
559 concentration in the ER and expanding the time for interaction, may also directly enhance
560 complex formation with HLA. As the proposed ER retention function impacts on complex
561 formation these two phenomena are interrelated and cannot be easily separated. Based on
562 the fact that polar amino acids rather interact with other polar TMDs (62), the polarity of the
563 E3/19K TMD is unlikely to directly mediate interaction with the non-polar TMD of HLA. Rather,
564 the E3/19K TMD may mediate self-association and this may be required for efficient HLA

565 complex formation. Accordingly, the E3/19K TMD may comprise the inner core of the complex
566 with the larger HLA molecule covering the exposed surface. In support of this, we consistently
567 observe efficient co-precipitation of E3/19K using mAbs against HLA, yet very little if any co-
568 precipitation of HLA when using E3/19K-specific mAbs. Oligomerisation may also be mediated
569 by cysteines as all E3/19K molecules have at least one cysteine in the TMD, and those of Ad
570 species B, C and E have 2-5 cysteines. Supporting this notion, we and others previously
571 provided evidence for the existence of disulfide-linked E3/19K dimers (13, 23, 28), although no
572 individual cysteine could be assigned to this phenomenon. For species D E3/19K,
573 oligomerization may also involve a GxxxG motif in their TMDs, which has been shown to serve
574 as a module to support interactions between TMD helices (63-65). Thus, the E3/19K TMD may
575 have an additional role in promoting oligomerization and thereby contribute to improved
576 complex formation with target molecules. Further mutagenesis analysis will be necessary to
577 clarify the role of these amino acids for oligomerisation and HLA or MICA/B down regulation.

578 It is not immediately obvious as to why two elements for ER localisation should be employed
579 for E3/19K function, as the di-lysine motif is highly efficacious and does not require an
580 additional element to ensure its ER localisation. However, our findings clearly show that
581 neither the ER retrieval signal on its own nor the TMD alone can provide complete suppression
582 of HLA and MICA/B cell surface levels. Given the efficiency of ER localisation by the ER retrieval
583 signal we suggest that the TMD of E3/19K has been evolutionary selected to maximize its
584 immunomodulatory function.

585 **Acknowledgements**

586 We are grateful to A. Steinle and G. Kettner for the gifts of antibodies, plasmids and Ad dl810.
587 We thank C. Ebenau-Jehle and A. Osterlehner for excellent technical assistance. We thank Dr.
588 Robert Spooner and Dr. Ann Dixon (University of Warwick) for critical reading of the
589 manuscript and helpful comments.

590 ## References

591 1. **Wold WSM, Horwitz MS.** 2007. Adenoviruses, p. 2395-2436. *In* Knipe DM, Howley PM,
592 Griffin DE, Lamb RA (ed.), Fields Virology, 5th ed. Lippincott Williams & Wilkins (LWW).

593 2. **Garnett CT, Talekar G, Mahr JA, Huang W, Zhang Y, Ornelles DA, Gooding LR.** 2009.
594 Latent species C adenoviruses in human tonsil tissues. J. Virol. **83:**2417-2428.

595 3. **Berk AJ.** 2007. Adenoviridae: The viruses and their replication, p. 2355-2394. *In* Knipe
596 DM, Howley PM, Griffin DE, Lamb RA (ed.), Fields Virology, Lippincott Williams &
597 Wilkins (LWW) ed.

598 4. **Burgert HG, Ruzsics Z, Obermeier S, Hilgendorf A, Windheim M, Elsing A.** 2002.
599 Subversion of host defense mechanisms by adenoviruses. Curr. Top. Microbiol.
600 Immunol. **269:**273-318.

601 5. **Echavarria M.** 2008. Adenoviruses in immunocompromised hosts. Clin. Microbiol. Rev.
602 **21:**704-715.

603 6. **Yamamoto M, Curiel DT.** 2010. Current issues and future directions of oncolytic
604 adenoviruses. Mol Ther **18:**243-250.

605 7. **Windheim M, Hilgendorf A, Burgert HG.** 2004. Immune evasion by adenovirus E3
606 proteins: exploitation of intracellular trafficking pathways. Curr. Top. Microbiol.
607 Immunol. **273:**29-85.

608 8. **Ginsberg HS, Lundholm-Beauchamp U, Horswood RL, Pernis B, Wold WS, Chanock**
609 **RM, Prince GA.** 1989. Role of early region 3 (E3) in pathogenesis of adenovirus disease.
610 Proc. Natl. Acad. Sci. U. S. A. **86:**3823-3827.

611 9. **Horwitz MS, Efrat S, Christen U, von Herrath MG, Oldstone MB.** 2009. Adenovirus E3
612 MHC inhibitory genes but not TNF/Fas apoptotic inhibitory genes expressed in beta
613 cells prevent autoimmune diabetes. Proc. Natl. Acad. Sci. U. S. A. **106:**19450-19454.
614 10. **Burgert HG, Blusch JH.** 2000. Immunomodulatory functions encoded by the E3
615 transcription unit of adenoviruses. Virus Genes **21:**13-25.
616 11. **McSharry BP, Burgert HG, Owen DP, Stanton RJ, Prod'homme V, Sester M, Koebernick**
617 **K, Groh V, Spies T, Cox S, Little AM, Wang EC, Tomasec P, Wilkinson GW.** 2008.
618 Adenovirus E3/19K promotes evasion of NK cell recognition by intracellular
619 sequestration of the NKG2D ligands major histocompatibility complex class I chain-
620 related proteins A and B. J. Virol. **82:**4585-4594.
621 12. **Burgert HG, Kvist S.** 1985. An adenovirus type 2 glycoprotein blocks cell surface
622 expression of human histocompatibility class I antigens. Cell **41:**987-997.
623 13. **Cox JH, Bennink JR, Yewdell JW.** 1991. Retention of adenovirus E19 glycoprotein in the
624 endoplasmic reticulum is essential to its ability to block antigen presentation. J. Exp.
625 Med. **174:**1629-1637.
626 14. **Burgert HG, Maryanski JL, Kvist S.** 1987. "E3/19K" protein of adenovirus type 2 inhibits
627 lysis of cytolytic T lymphocytes by blocking cell-surface expression of histocompatibility
628 class I antigens. Proc. Natl. Acad. Sci. U. S. A. **84:**1356-1360.
629 15. **Hansen TH, Bouvier M.** 2009. MHC class I antigen presentation: learning from viral
630 evasion strategies. Nat Rev Immunol **9:**503-513.
631 16. **Jonjic S, Babic M, Polic B, Krmpotic A.** 2008. Immune evasion of natural killer cells by
632 viruses. Curr. Opin. Immunol. **20:**30-38.

633 17. **Deryckere F, Burgert HG.** 1996. Early region 3 of adenovirus type 19 (subgroup D)
634 encodes an HLA-binding protein distinct from that of subgroups B and C. J Virol
635 **70:**2832-2841.
636 18. **Flomenberg P, Szmulewicz J, Gutierrez E, Lupatkin H.** 1992. Role of the adenovirus E3-
637 19k conserved region in binding major histocompatibility complex class I molecules. J.
638 Virol. **66:**4778-4783.
639 19. **Nilsson T, Jackson M, Peterson PA.** 1989. Short cytoplasmic sequences serve as
640 retention signals for transmembrane proteins in the endoplasmic reticulum. Cell
641 **58:**707-718.
642 20. **Jackson MR, Nilsson T, Peterson PA.** 1990. Identification of a consensus motif for
643 retention of transmembrane proteins in the endoplasmic reticulum. EMBO J. **9:**3153-
644 3162.
645 21. **Jackson MR, Nilsson T, Peterson PA.** 1993. Retrieval of transmembrane proteins to the
646 endoplasmic reticulum. J. Cell Biol. **121:**317-333.
647 22. **Liu H, Fu J, Bouvier M.** 2007. Allele- and locus-specific recognition of class I MHC
648 molecules by the immunomodulatory E3-19K protein from adenovirus. J. Immunol.
649 **178:**4567-4575.
650 23. **Sester M, Burgert HG.** 1994. Conserved cysteine residues within the E3/19K protein of
651 adenovirus type 2 are essential for binding to major histocompatibility complex
652 antigens. J. Virol. **68:**5423-5432.
653 24. **Sester M, Koebernick K, Owen D, Ao M, Bromberg Y, May E, Stock E, Andrews L, Groh**
654 **V, Spies T, Steinle A, Menz B, Burgert HG.** 2010. Conserved amino acids within the
655 adenovirus 2 E3/19K protein differentially affect downregulation of MHC class I and
656 MICA/B proteins. J. Immunol. **184:**255-267.

657 25. **Fu J, Li L, Bouvier M.** 2011. Adenovirus E3-19K proteins of different serotypes and
658 subgroups have similar, yet distinct, immunomodulatory functions toward major
659 histocompatibility class I molecules. J. Biol. Chem. **286:**17631-17639.
660 26. **Li L, Muzahim Y, Bouvier M.** 2012. Crystal structure of adenovirus E3-19K bound to
661 HLA-A2 reveals mechanism for immunomodulation. Nat Struct Mol Biol **19:**1176-1181.
662 27. **Liu H, Stafford WF, Bouvier M.** 2005. The endoplasmic reticulum lumenal domain of
663 the adenovirus type 2 E3-19K protein binds to peptide-filled and peptide-deficient HLA-
664 A*1101 molecules. J Virol **79:**13317-13325.
665 28. **Pääbo S, Weber F, Nilsson T, Schaffner W, Peterson PA.** 1986. Structural and functional
666 dissection of an MHC class I antigen-binding adenovirus glycoprotein. EMBO J. **5:**1921-
667 1927.
668 29. **Pääbo S, Bhat BM, Wold WS, Peterson PA.** 1987. A short sequence in the COOH-
669 terminus makes an adenovirus membrane glycoprotein a resident of the endoplasmic
670 reticulum. Cell **50:**311-317.
671 30. **Gabathuler R, Kvist S.** 1990. The endoplasmic reticulum retention signal of the E3/19K
672 protein of adenovirus type 2 consists of three separate amino acid segments at the
673 carboxy terminus. J. Cell Biol. **111:**1803-1810.
674 31. **Gabathuler R, Levy F, Kvist S.** 1990. Requirements for the association of adenovirus
675 type 2 E3/19K wild-type and mutant proteins with HLA antigens. J. Virol. **64:**3679-3685.
676 32. **Teasdale RD, Jackson MR.** 1996. Signal-mediated sorting of membrane proteins
677 between the endoplasmic reticulum and the golgi apparatus. Annu. Rev. Cell Dev. Biol.
678 **12:**27-54.

679 33. **Zerangue N, Malan MJ, Fried SR, Dazin PF, Jan YN, Jan LY, Schwappach B.** 2001.
680 Analysis of endoplasmic reticulum trafficking signals by combinatorial screening in
681 mammalian cells. Proc. Natl. Acad. Sci. U.S.A **98:**2431-2436.
682 34. **Lapham CK, Bacik I, Yewdell JW, Kane KP, Bennink JR.** 1993. Class I molecules retained
683 in the endoplasmic reticulum bind antigenic peptides. J Exp Med **177:**1633-1641.
684 35. **Kvist S, Roberts L, Dobberstein B.** 1983. Mouse histocompatibility genes: structure and
685 organisation of a Kd gene. EMBO J. **2:**245-254.
686 36. **Sester M, Feuerbach D, Frank R, Preckel T, Gutermann A, Burgert HG.** 2000. The
687 amyloid precursor-like protein 2 associates with the major histocompatibility complex
688 class I molecule K(d). J. Biol. Chem. **275:**3645-3654.
689 37. **Körner H, Fritzsche U, Burgert HG.** 1992. Tumor necrosis factor alpha stimulates
690 expression of adenovirus early region 3 proteins: implications for viral persistence.
691 Proc. Natl. Acad. Sci. U. S. A. **89:**11857-11861.
692 38. **Ruzsics Z, Wagner M, Osterlehner A, Cook J, Koszinowski U, Burgert HG.** 2006.
693 Transposon-assisted cloning and traceless mutagenesis of adenoviruses: Development
694 of a novel vector based on species D. J Virol **80:**8100-8113.
695 39. **Hilgendorf A, Lindberg J, Ruzsics Z, Honing S, Elsing A, Lofqvist M, Engelmann H,**
696 **Burgert HG.** 2003. Two distinct transport motifs in the adenovirus E3/10.4-14.5
697 proteins act in concert to down-modulate apoptosis receptors and the epidermal
698 growth factor receptor. J. Biol. Chem. **278:**51872-51884.
699 40. **Parham P, Brodsky FM.** 1981. Partial purification and some properties of BB7.2. A
700 cytotoxic monoclonal antibody with specificity for HLA-A2 and a variant of HLA-A28.
701 Hum Immunol **3:**277-299.

702 41. **Welte SA, Sinzger C, Lutz SZ, Singh-Jasuja H, Sampaio KL, Eknigk U, Rammensee HG,**
703 **Steinle A.** 2003. Selective intracellular retention of virally induced NKG2D ligands by the
704 human cytomegalovirus UL16 glycoprotein. Eur. J. Immunol. **33:**194-203.
705 42. **Menz B, Sester M, Koebernick K, Schmid R, Burgert HG.** 2008. Structural analysis of the
706 adenovirus type 2 E3/19K protein using mutagenesis and a panel of conformation-
707 sensitive monoclonal antibodies. Mol. Immunol. **46:**16-26.
708 43. **Burgert HG, Kvist S.** 1987. The E3/19K protein of adenovirus type 2 binds to the
709 domains of histocompatibility antigens required for CTL recognition. EMBO J. **6:**2019-
710 2026.
711 44. **Windheim M, Burgert HG.** 2002. Characterization of E3/49K, a novel, highly
712 glycosylated E3 protein of the epidemic keratoconjunctivitis-causing adenovirus type
713 19a. J. Virol. **76:**755-766.
714 45. **Lapham CK, Bacik I, Yewdell JW, Kane KP, Bennink JR.** 1993. Class I molecules retained
715 in the endoplasmic reticulum bind antigenic peptides. J. Exp. Med **177:**1633-1641.
716 46. **Ellgaard L, Helenius A.** 2003. Quality control in the endoplasmic reticulum. Nat. Rev.
717 Mol. Cell Biol. **4:**181-191.
718 47. **Kornfeld R, Wold WS.** 1981. Structures of the oligosaccharides of the glycoprotein
719 coded by early region E3 of adenovirus 2. J. Virol. **40:**440-449.
720 48. **Beier DC, Cox JH, Vining DR, Cresswell P, Engelhard VH.** 1994. Association of human
721 class I MHC alleles with the adenovirus E3/19K protein. J. Immunol. **152:**3862-3872.
722 49. **Berg M, Difatta J, Hoiczyk E, Schlegel R, Ketner G.** 2005. Viable adenovirus vaccine
723 prototypes: high-level production of a papillomavirus capsid antigen from the major
724 late transcriptional unit. Proc Natl Acad Sci U S A **102:**4590-4595.

725 50. **Hermiston TW, Tripp RA, Sparer T, Gooding LR, Wold WS.** 1993. Deletion mutation
726 analysis of the adenovirus type 2 E3-gp19K protein: identification of sequences within
727 the endoplasmic reticulum lumenal domain that are required for class I antigen binding
728 and protection from adenovirus-specific cytotoxic T lymphocytes. J. Virol. **67:**5289-
729 5298.
730 51. **Pääbo S, Nilsson T, Peterson PA.** 1986. Adenoviruses of subgenera B, C, D, and E
731 modulate cell-surface expression of major histocompatibility complex class I antigens.
732 Proc. Natl. Acad. Sci. U. S. A. **83:**9665-9669.
733 52. **Lankford SP, Cosson P, Bonifacino JS, Klausner RD.** 1993. Transmembrane domain
734 length affects charge-mediated retention and degradation of proteins within the
735 endoplasmic reticulum. J Biol Chem **268:**4814-4820.
736 53. **Hennecke S, Cosson P.** 1993. Role of transmembrane domains in assembly and
737 intracellular transport of the CD8 molecule. J Biol Chem **268:**26607-26612.
738 54. **Deryckere F, Burgert HG.** 1996. Tumor necrosis factor alpha induces the adenovirus
739 early 3 promoter by activation of NF-kappaB. J Biol Chem **271:**30249-30255.
740 55. **Cherayil BJ, MacDonald K, Waneck GL, Pillai S.** 1993. Surface transport and
741 internalization of the membrane IgM H chain in the absence of the Mb-1 and B29
742 proteins. J. Immunol. **151:**11-19.
743 56. **Williams GT, Venkitaraman AR, Gilmore DJ, Neuberger MS.** 1990. The sequence of the
744 mu transmembrane segment determines the tissue specificity of the transport of
745 immunoglobulin M to the cell surface. J. Exp. Med. **171:**947-952.
746 57. **Murakami K, Mihara K, Omura T.** 1994. The transmembrane region of microsomal
747 cytochrome P450 identified as the endoplasmic reticulum retention signal. J Biochem
748 **116:**164-175.

749 58. **Szczesna-Skorupa E, Ahn K, Chen CD, Doray B, Kemper B.** 1995. The cytoplasmic and
750 N-terminal transmembrane domains of cytochrome P450 contain independent signals
751 for retention in the endoplasmic reticulum. J. Biol. Chem. **270:**24327-24333.
752 59. **Barre L, Magdalou J, Netter P, Fournel-Gigleux S, Ouzzine M.** 2005. The stop transfer
753 sequence of the human UDP-glucuronosyltransferase 1A determines localization to the
754 endoplasmic reticulum by both static retention and retrieval mechanisms. FEBS J
755 **272:**1063-1071.
756 60. **Cocquerel L, Duvet S, Meunier JC, Pillez A, Cacan R, Wychowski C, Dubuisson J.** 1999.
757 The transmembrane domain of hepatitis C virus glycoprotein E1 is a signal for static
758 retention in the endoplasmic reticulum. J. Virol. **73:**2641-2649.
759 61. **Hobman TC, Lemon HF, Jewell K.** 1997. Characterization of an endoplasmic reticulum
760 retention signal in the rubella virus E1 glycoprotein. J Virol **71:**7670-7680.
761 62. **Dixon AM, Stanley BJ, Matthews EE, Dawson JP, Engelman DM.** 2006. Invariant chain
762 transmembrane domain trimerization: a step in MHC class II assembly. Biochemistry
763 **45:**5228-5234.
764 63. **Moore DT, Berger BW, DeGrado WF.** 2008. Protein-Protein Interactions in the
765 Membrane: Sequence, Structural, and Biological Motifs. Structure **16:**991-1001.
766 64. **Unterreitmeier S, Fuchs A, Schaffler T, Heym RG, Frishman D, Langosch D.** 2007.
767 Phenylalanine promotes interaction of transmembrane domains via GxxxG motifs. J.
768 Mol. Biol. **374:**705-718.
769 65. **Langosch D, Arkin IT.** 2009. Interaction and conformational dynamics of membrane-
770 spanning protein helices. Protein Sci. **18:**1343-1358.

771

772 ## Figure legends

773 **FIGURE 1: Schematic representation of wild-type E3/19K (EEE), murine MHC-I K^d (KKK) and**
774 **various chimeric proteins.** The composition of the chimera is indicated on the left by three
775 capital letters representing the ER luminal, transmembrane and cytoplasmic domains,
776 respectively. An 'E' refers to E3/19K-derived sequences (white boxes), and a 'K' to K^d-specific
777 sequences (grey boxes). Asterisks (*) denote mutation of the di-lysine motif. All constructs
778 were stably transfected into the human embryonic kidney cell line 293.

779 **FIGURE 2: Differential cell surface and intracellular distribution of mutant constructs in 293**
780 **cells stably expressing K^d, wild-type E3/19K and E3/19K variants.** Internal and cell surface
781 expression of constructs was determined by quantitative flow cytometry in the presence and
782 absence of saponin, respectively. MHC-I K^d was detected using mAb 34-1-2, wild-type E3/19K
783 and E3/19K mutants were detected using mAb Tw1.3. **(A)** Filled histograms represent the
784 background staining obtained with the secondary antibody alone, the open histograms denote
785 specific staining. The mean fluorescence intensity (MFI) is given in the upper right corner of
786 each histogram. **(B)** The cellular distribution is expressed as the ratio of the MFIs obtained
787 upon cell surface and internal staining. At least three independent experiments were
788 performed from at least three different clones of EEE*, EEK, EKK, EKE* and EKE, two cell lines
789 for EEE, and one cell line for KKK. Data are expressed as mean and standard error of the mean.

790 **FIGURE 3: Subcellular distribution of wild-type E3/19K and E3/19K mutants as analysed by**
791 **immunofluorescence.** Transfected 293 cells stably expressing wild-type E3/19K (EEE), EEE*,
792 EEK, EKK, EKE* and EKE were stained for immunofluorescence microscopy using mAb 3A9

793 followed by Cy3-conjugated goat anti-mouse IgG. Cells were left intact to assess cell surface
794 expression **(A–F)** or were permeabilized with Triton-X-100 for internal staining **(G–L)**.

795 **FIGURE 4: Size and carbohydrate modification of wild-type E3/19K and E3/19K variants as**
796 **analysed by immunoprecipitation. (A)** E3/19K constructs were immunoprecipitated from
797 lysates of stably transfected cell lines after 1 hour of metabolic labeling with ^{35}S-methionine
798 using mAb Tw1.3 directed to a conformational epitope in the luminal domain of E3/19K.
799 Similar results were obtained after immunoprecipitation with the conformation-dependent
800 mAbs 3A9 and 3F4 (data not shown). The black arrowheads indicate monoglycosylated forms
801 of E3/19K. **(B)** E3/19K wild type (EEE) and EEK constructs were immunoprecipitated from
802 lysates of stably transfected 293 and K562 cell lines after 2.5 hours of metabolic labeling with
803 ^{35}S-methionine using mAb Tw1.3. Acquisition of complex type glycans is visualized as slower
804 migrating protein species above the main labelled band (denoted by a line and asterisk on the
805 right site of the respective lane in panels B and C). **(C)** K562 cells and transfectants with wild
806 type E3/19K and EEK were pulse labelled for 20 minutes and chased for 1 and 3 hours.
807 Precipitated material was treated with endo H to identify constructs that still contain high
808 mannose carbohydrates that are cleaved by endo H (^{c}) and therefore have not been
809 transported through the medial Golgi. The numbers on the left denote the positions of the
810 molecular weight marker proteins of 46kDa and 30kDa.

811 **FIGURE 5: E3/19K constructs exhibit a differential complex formation with HLA.** 293 cells and
812 cell clones stably expressing E3/19K constructs were metabolically labelled with ^{35}S-
813 methionine for 1h and lysates were subjected to immunoprecipitation with mAb W6/32. **(A)**
814 The positions of HLA-I heavy chains (HLA), the various E3/19K forms (EXX) and β_2-microglobulin

815 (β_2m) are marked on the right, those of molecular weight markers (kDa) are indicated on the
816 left. **(B)** The association with HLA-I of wild-type E3/19K and mutants shown in panel A was
817 quantitatively assessed by measuring the amount of radioactive E3/19K co-precipitated with
818 HLA and relating it to the total amount expressed as detected by direct precipitation with
819 Tw1.3 using a phosphoimager (data not shown). The ability of the different mutants to bind to
820 HLA-I is expressed as the ratio of radioactivity detected in the co-precipitated versus directly
821 precipitated E3/19K band. The ratio obtained for wild-type E3/19K was set to 100%. The data
822 are from a single coprecipitation experiment.

823 **FIGURE 6: Differential transport of HLA molecules in cells expressing the E3/19K chimera.**
824 Transport of HLA molecules was analysed in a pulse-chase experiment (20 min pulse, 2.5 h
825 chase). Firstly, HLA-A2 was immunoprecipitated with mAb BB7.2 **(A).** The remaining HLA-A, -B,
826 -C molecules were precipitated with mAb W6/32 **(B)**. Precipitated material was treated with
827 endo H to enable differentiation between molecules transported through the medial Golgi
828 apparatus where these acquire endo H resistant (^{R}) complex type carbohydrates and those that
829 still contain high mannose carbohydrates and are cleaved by endo H (^{c}) and therefore have not
830 reached this compartment. The percentage of HLA molecules that had acquired endo H
831 resistance (% endo H resistant) relative to the total amount of HLA precipitated is shown
832 separately in corresponding bar diagrams for HLA-A2 **(A)** and the remaining HLA molecules **(B)**.

833 **FIGURE 7: Relative cell surface expression of the E3/19K target molecules HLA and MICA/B in**
834 **cell clones expressing mutant and wild-type E3/19K.** Steady state cell surface expression of
835 HLA **(A)** and MICA/B **(B)** was determined by flow cytometry using mAb W6/32 and BAMO3,
836 respectively, followed by incubation with Alexa 488 coupled goat anti-mouse IgG. At least

837 three clones of each transfection were analysed in at least two independent experiments. The
838 background staining obtained with the secondary antibody alone was subtracted and the mean
839 fluorescence intensity (MFI) related to that of 293 cells and three E3/19K negative transfectant
840 clones (293) which was set to 100%. Bars represent mean values and standard error of the
841 mean.

842 **FIGURE 8: The E3/19K TMD confers ER retention to the bona-fide cell surface molecule,**
843 **MHC–I K^d.** The TMD of MHC-I K^d (KKK) was replaced by that of E3/19K yielding KEK. (A) The
844 identity of the KEK domain structure was verified by successful immunoprecipitation with
845 antibodies against the luminal domain and the respective cytoplasmic tail. Detergent extracts
846 of various control cell lines and 293 cells stably expressing KEK were immunoprecipitated using
847 either a mAb to the luminal $\alpha1/\alpha2$ domains of K^d (34-1-2, left) or an antiserum against the
848 cytoplasmic tail (αK^d C-tail, right). 293 cells and K1, a G418 resistant, KEK negative clone,
849 served as negative controls. In addition, cell lines stably expressing wild-type K^d (KKK; $293K^d2$)
850 or both wild-type K^d and E3/19K (KKK+EEE; $29312K^d8$), were analysed. The position of K^d, KEK,
851 β_2m, E3/19K, APLP2 and an unidentified protein (arrow) are indicated on the right, that of
852 molecular weight markers (kDa) on the left. **(B)** KEK expression on the cell surface is similar to
853 that of MHC-I K^d in the presence of wild-type E3/19K. 293 cells transfected with KKK+EEE, KKK,
854 KEK or KKE were analyzed as before by flow cytometry using mAb 34-1-2 in the presence and
855 absence of saponin. The ratio of the surface versus internal expression was calculated. The
856 bars represent the mean and standard error of the mean derived from at least 3 independent
857 experiments. Similar data were obtained using mAb SF1.1.1 directed against the $\alpha3$ domain of
858 K^d (data not shown). **(C)** The processing pattern and enhanced co-precipitation of APLP2
859 (100/110 kDa) by KEK indicates ER retention. 293 cells stably expressing KEK, KKE and wild-type

860 K^d in the absence (KKK; 293K^d2) and presence of E3/19K (KKK+EEE; 293.12K^d8) were pulse-
861 labelled for 20 min (0) and then chased for 40 min and 120 min as indicated. The annotation is
862 as in 8A. The asterisk in lane 6 indicates K^d species with complex-type carbohydrates. Note the
863 enhanced co-precipitation of APLP2 (p100/110 bands) in cells expressing KKK+EEE, KEK, and
864 KKE as compared to cells expressing wild-type K^d alone (KKK), which is indicative of ER
865 retention (36).

866 **FIGURE 9: The cell surface and intracellular distribution of E3/19K variants and HLA is**
867 **confirmed in the context of virus infection.** The E3/19K mutants EEE*, EKE and EKE* were
868 inserted in the Ad2 genome by recombineering and reconstituted viruses were used to infect
869 293 cells. Cells were analyzed 18h post infection by flow cytometry for cell surface and internal
870 expression of E3/19K constructs and HLA using mAbs Tw1.3 and W6/32, respectively. The ratio
871 of cell surface versus internal staining of E3/19K constructs **(A)** and HLA **(B)** is given as mean
872 and standard error of the mean derived from three independent experiments. Similar results
873 were obtained upon infection of HeLa cells (data not shown).

874 **FIGURE 10: Summary of transport characteristics of wild-type E3/19K and chimera, and their**
875 **effect on HLA transport in transfected cells.** Transport of E3/19K constructs and HLA
876 molecules between the ER and the ERGIC/*cis*-Golgi complex and from there to the plasma
877 membrane is indicated by black and grey arrows, respectively. The thickness of the arrows
878 represents the intensity of transport. Mutants are grouped in panels **A**-**D** according to their
879 transport behaviour. The capacity for static ER retention and the extent of HLA down
880 regulation is semiquantitatively indicated on the left and right side, respectively.

881

Figure 1

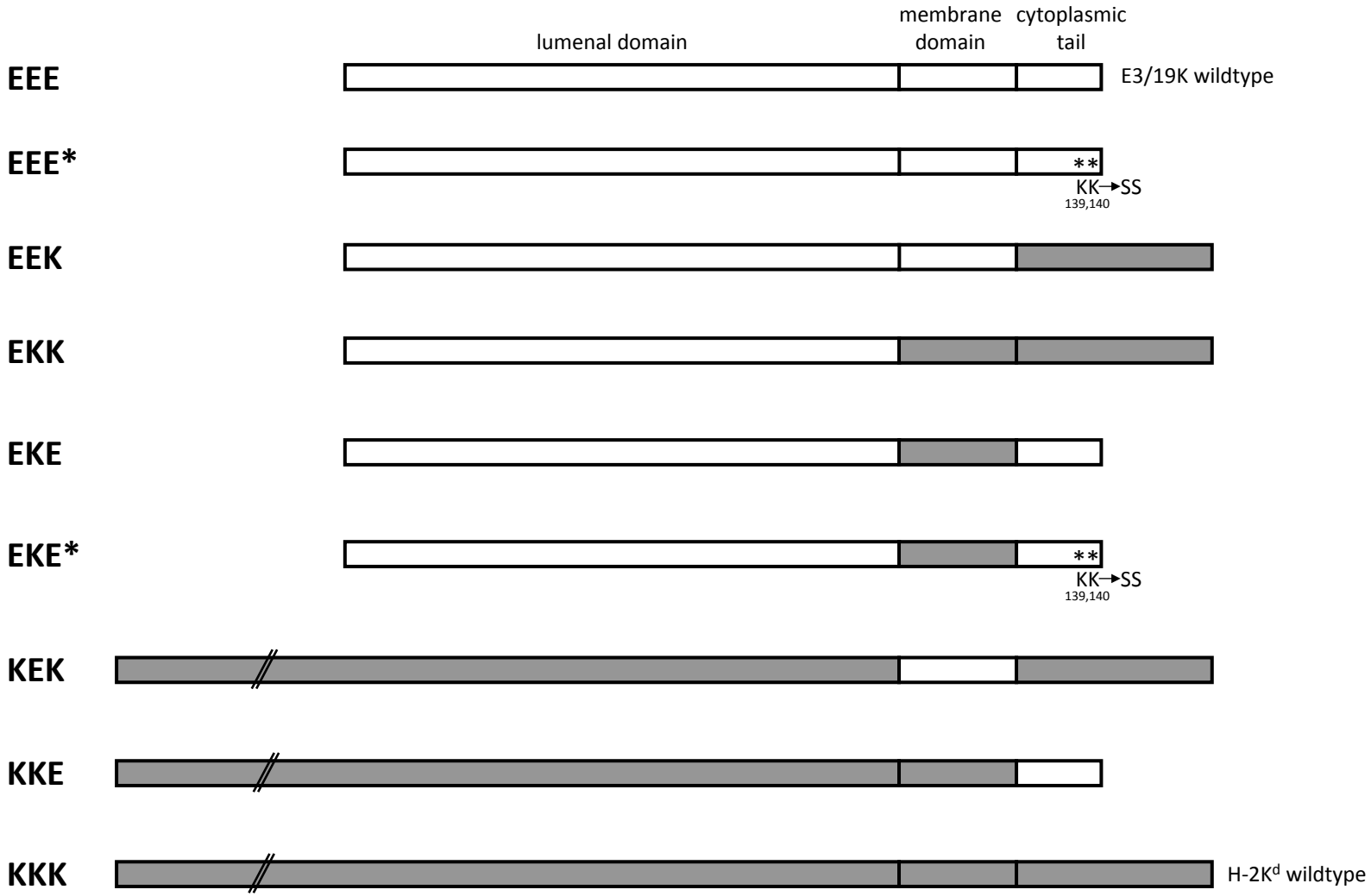
lumenal domain
membrane domain
cytoplasmic tail
EEE
E3/19K wildtype
EEE*
**
KK→SS
139,140
EEK
EKK
EKE
EKE*
**
KK→SS
139,140
KEK
KKE
KKK
H-2K^d wildtype

Figure 2

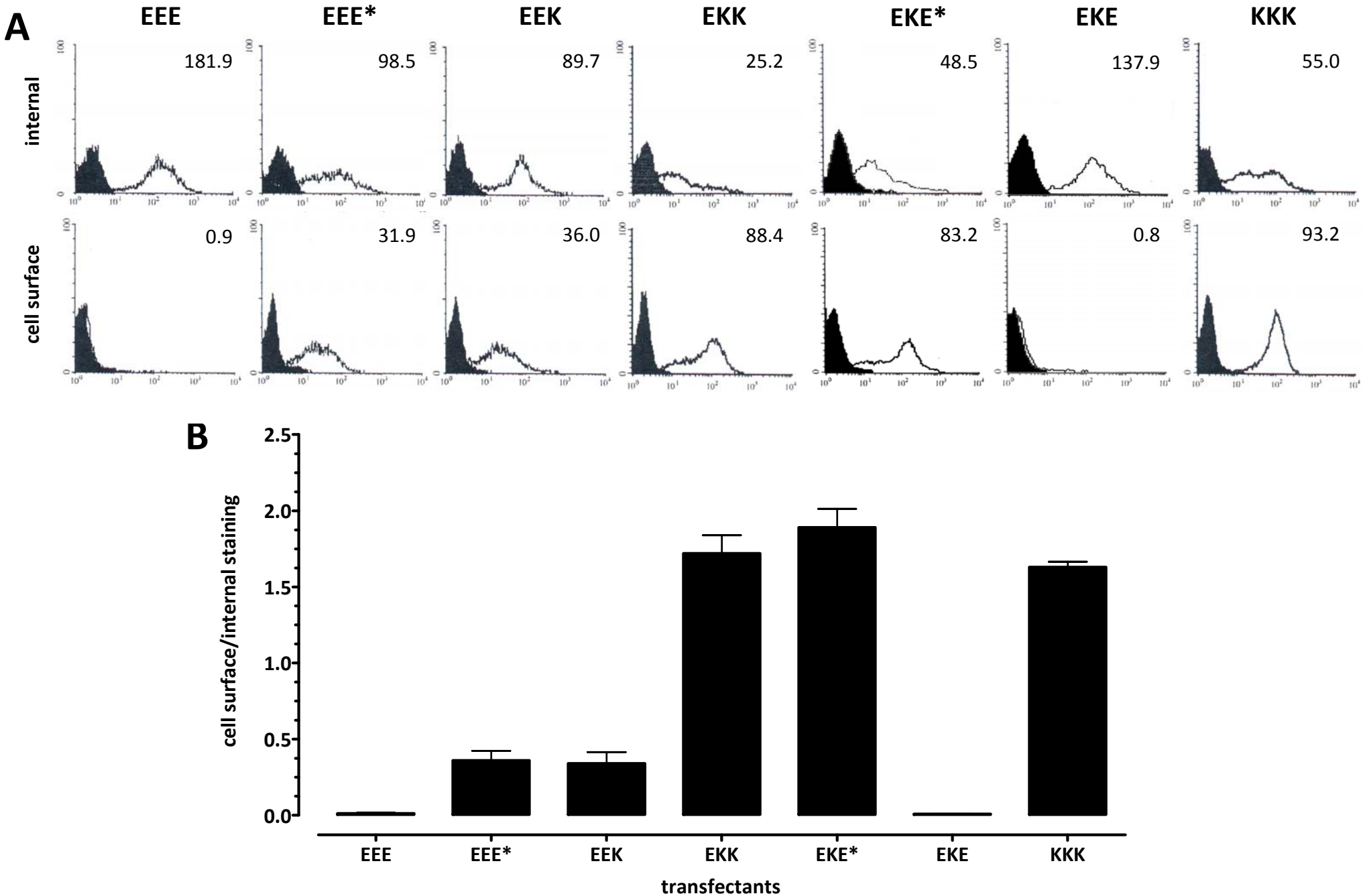
A
EEE
EEE*
EEK
EKK
EKE*
EKE
KKK
internal
cell surface
181.9
98.5
89.7
25.2
48.5
137.9
55.0
0.9
31.9
36.0
88.4
83.2
0.8
93.2
B
cell surface/internal staining
2.5
2.0
1.5
1.0
0.5
0.0
EEE
EEE*
EEK
EKK
EKE*
EKE
KKK
transfectants

Figure 3

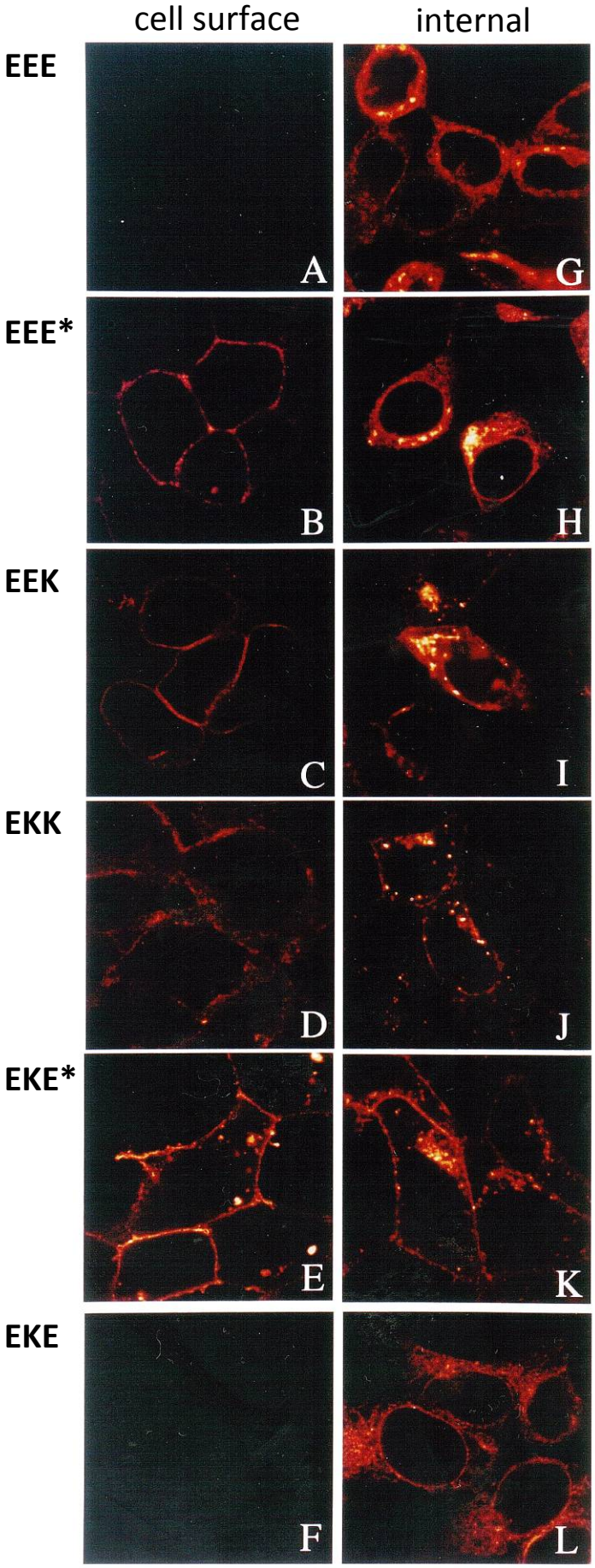

Figure 4

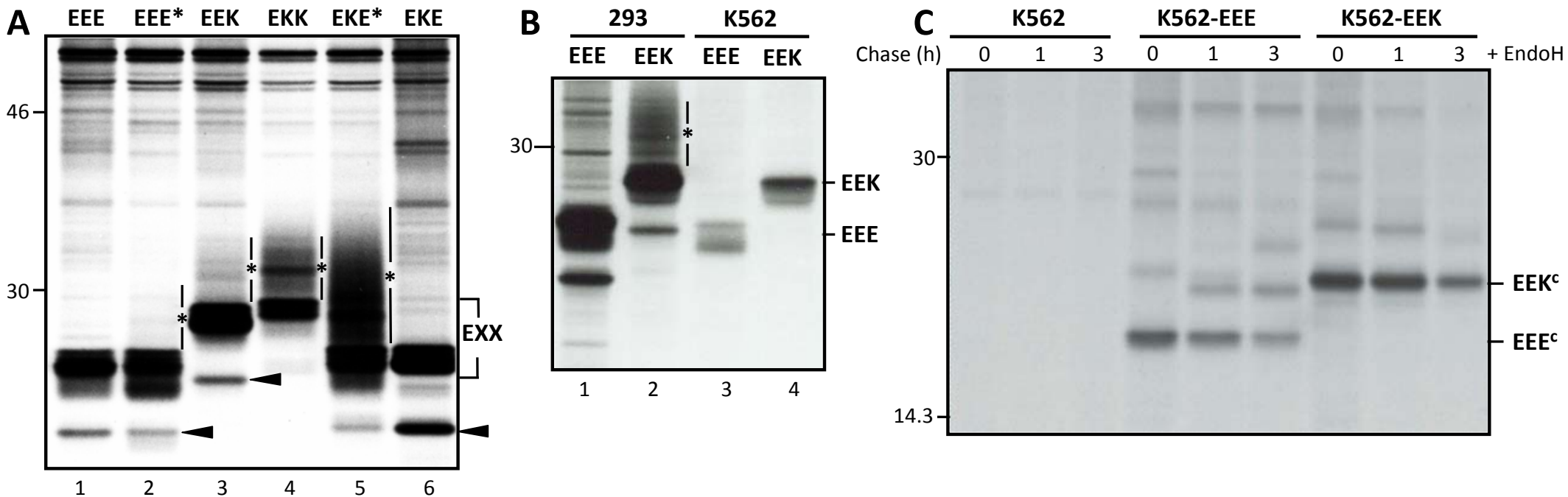
A
EEE
EEE*
EEK
EKK
EKE*
EKE
46
30
EXX
1
2
3
4
5
6
B
293
K562
EEE
EEK
EEE
EEK
30
EEK
EEE
1
2
3
4
C
K562
K562-EEE
K562-EEK
Chase (h)
0
1
3
0
1
3
0
1
3
+ EndoH
30
14.3
EEK^c
EEE^c

Figure 5

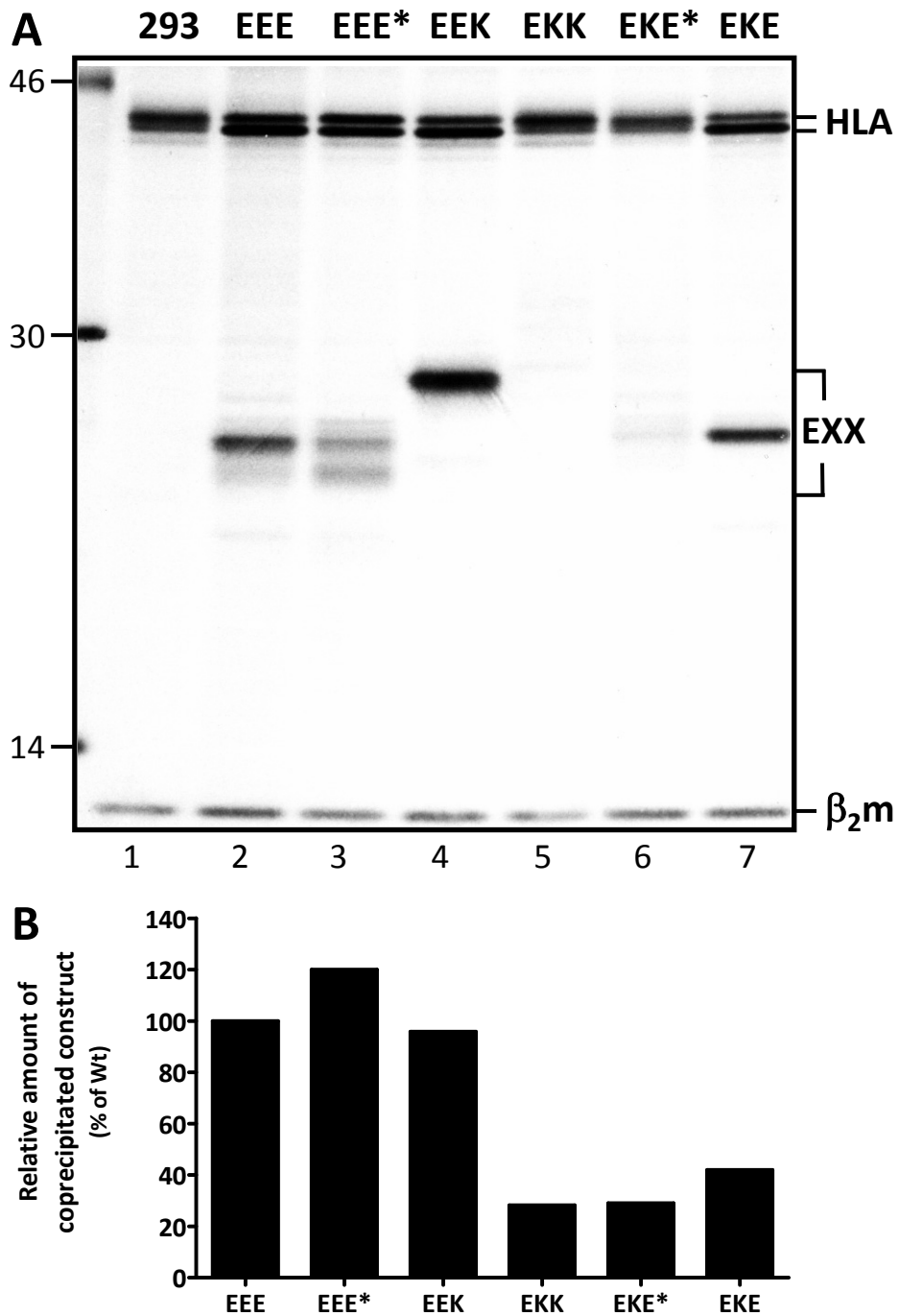
A
293
EEE
EEE*
EEK
EKK
EKE*
EKE
46
30
14
HLA
EXX
β2m
1
2
3
4
5
6
7
B
Relative amount of coprecipitated construct (% of Wt)
140
120
100
80
60
40
20
0
EEE
EEE*
EEK
EKK
EKE*
EKE

Figure 6

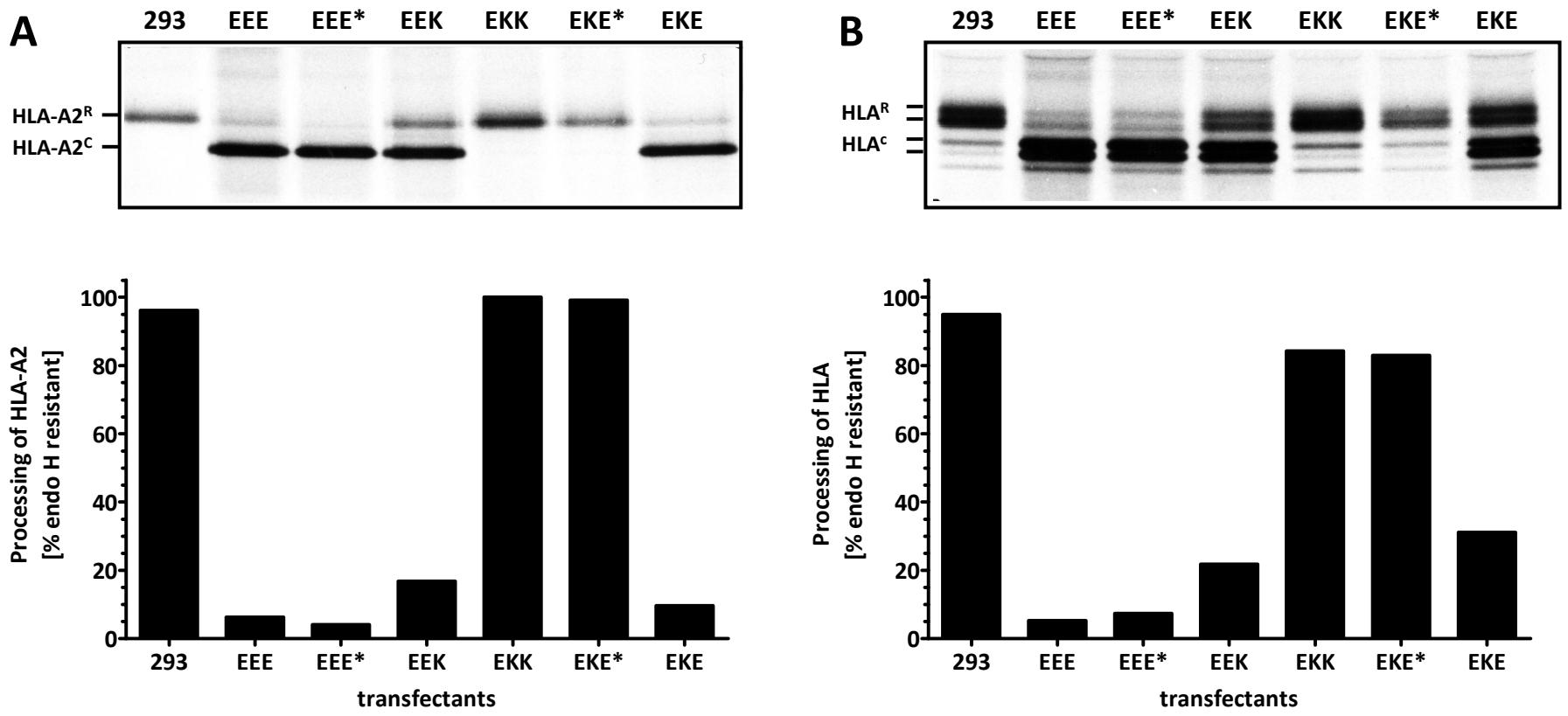
A
293
EEE
EEE*
EEK
EKK
EKE*
EKE
HLA-A2R
HLA-A2C
Processing of HLA-A2
[% endo H resistant]
100
80
60
40
20
0
transfectants
B
HLAR
HLAc
Processing of HLA
[% endo H resistant]

Figure 7

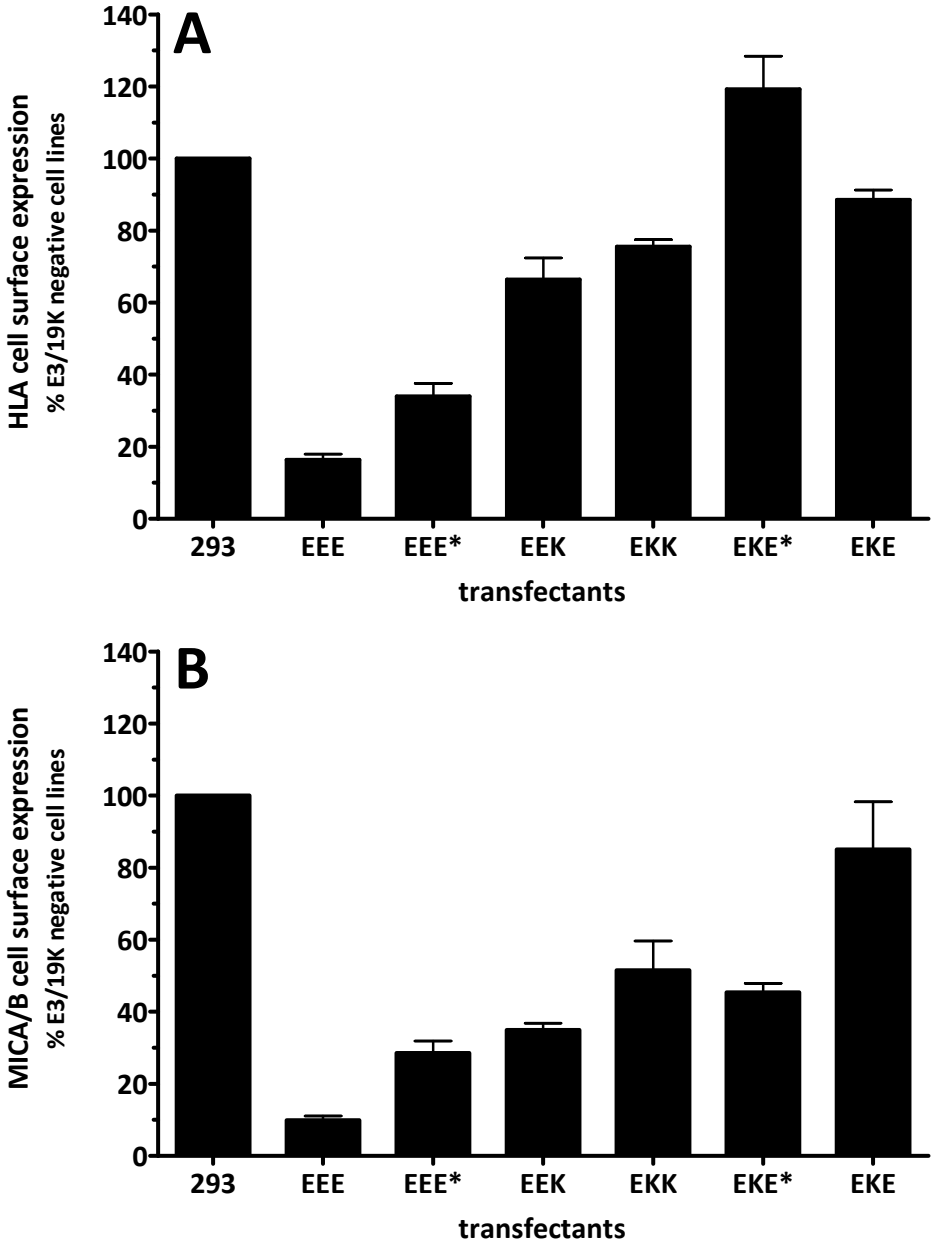
A
HLA cell surface expression
% E3/19K negative cell lines
140
120
100
80
60
40
20
0
293
EEE
EEE*
EEK
EKK
EKE*
EKE
transfectants
B
MICA/B cell surface expression
% E3/19K negative cell lines
140
120
100
80
60
40
20
0
293
EEE
EEE*
EEK
EKK
EKE*
EKE
transfectants

Figure 8

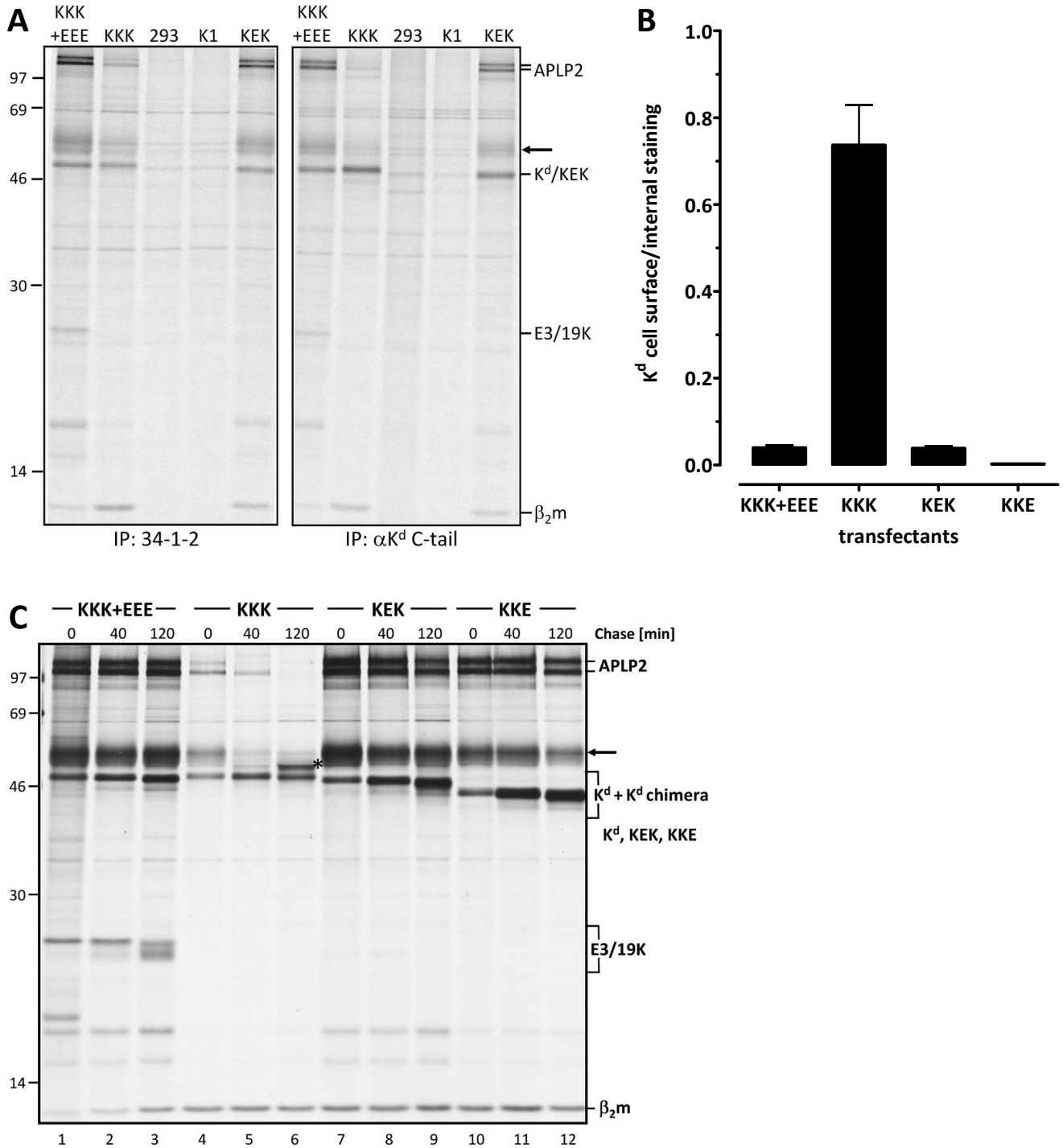
A
KKK +EEE
KKK
293
K1
KEK
97
69
46
30
14
APLP2
Kd/KEK
E3/19K
β2m
IP: 34-1-2
IP: αKd C-tail
B
Kd cell surface/internal staining
1.0
0.8
0.6
0.4
0.2
0.0
KKK+EEE
KKK
KEK
KKE
transfectants
C
KKK+EEE
KKK
KEK
KKE
0
40
120
Chase [min]
APLP2
Kd + Kd chimera
Kd, KEK, KKE
E3/19K
β2m
1
2
3
4
5
6
7
8
9
10
11
12

Figure 9

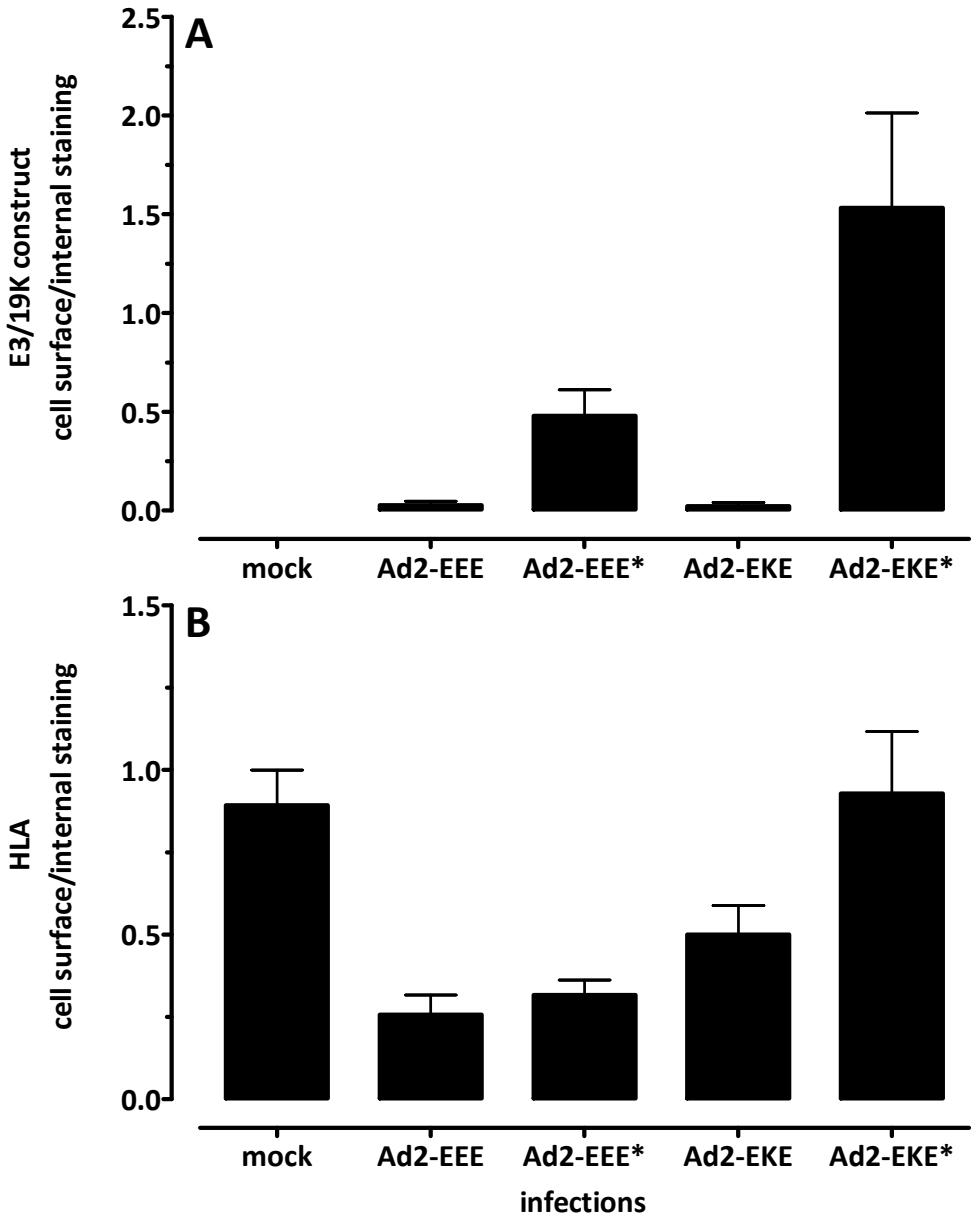
A
E3/19K construct
cell surface/internal staining
2.5
2.0
1.5
1.0
0.5
0.0
mock
Ad2-EEE
Ad2-EEE*
Ad2-EKE
Ad2-EKE*
B
HLA
cell surface/internal staining
1.5
1.0
0.5
0.0
mock
Ad2-EEE
Ad2-EEE*
Ad2-EKE
Ad2-EKE*
infections

Figure 10

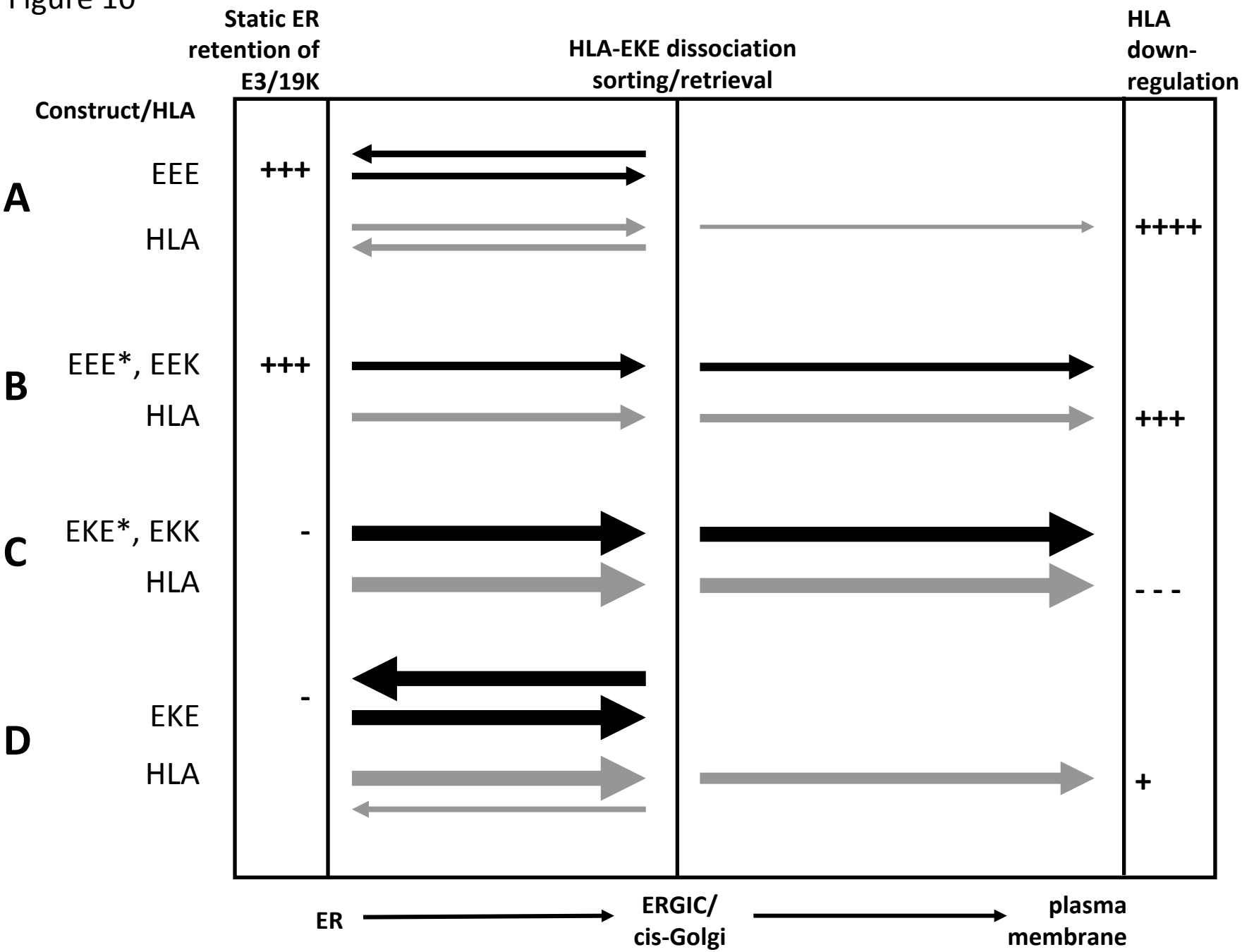
Static ER retention of E3/19K
HLA-EKE dissociation sorting/retrieval
HLA down-regulation
Construct/HLA
A
EEE
+++
HLA
++++
B
EEE*, EEK
+++
HLA
+++
C
EKE*, EKK
-
HLA
- - -
D
EKE
-
HLA
+
ER
ERGIC/ cis-Golgi
plasma membrane